THE EFFECT OF END FIXITY ON THE

STABILITY OF STRUCTURES

A THESIS

Presented to

The Faculty of the Division of Graduate

Studies and Research

by

Takaya Iwamoto

In Partial Fulfillment

of the Requirements for the Degree

Doctor of Philosophy

in the School of Aerospace Engineering

Georgia Institute of Technology

September, 1970

THE EFFECT OF END FIXITY ON THE
STABILITY OF STRUCTURES

Approved:

_____

Chairman

_____

_____

_____

Date Approved by Chairman: 24 May 1973.

ACKNOWLEDGMENTS

TABLE OF CONTENTS

Introduction of the Uniformly Distributed Load
Search for the Empirical Laws
Generalization to the Case of a Moving Lateral Support
Non-Uniform Cross Section

Formulation of the Integral Equation
Orthogonality Relations
Some Useful Results Derived from the Integral Equation
    Formulation
Application and Discussions of the Results Obtained in
    Section 3

TABLE OF CONTENTS (Continued)

LIST OF TABLES

LIST OF ILLUSTRATIONS

LIST OF SYMBOLS

A, B, C, D,	constants of integration
C	flexibility influence function
$\vec{C}$	C/L
E	modulus of the material
h	size of division used in finite difference solution
I	second moment of area
i	a digit, 1, 2, 3, etc.
j	a digit, 1, 2, 3, etc.
K_1, K_2	spring stiffnesses for rotational restraint
K_3, K_4	spring stiffnesses for lateral restraint
k	$\sqrt{P/EI}$
L	column or beam length
$\bar{L}$	distance between points of zero shearing force
l_{ext}	distance apart of inflexion points
l_1, l_2	distance of the column end from furthermost inflexion point
l_{max}	the greater of l_1 and l_2
M	bending moment
N	number of discrete lateral loads on a beam
N_i	$\int_0^1 \theta_i^2 (x)\, dx$
n	number of unknown points within the span of the beam
P	axial load
P_{cr}	critical value of P
p	positive number which defines taper law, $(EI(x) = EI_0 \{1 - 1/T\ (x/L)^p\})$

Q	concentrated lateral load
q	intensity of distributed lateral loads
$\bar{q}$	non-dimensional lateral load parameters $= qL^3/EI$
T	taper ratio of the bending stiffness
U	an energy function
V	shearing force
W	lateral deflection
W_e	work done by axial force P
w	non-dimensional deflection parameter $= W/L$
X	coordinate along beam or column
x	non-dimensional coordinate $= X/L$
Z	$\alpha_0 - \alpha_1$ a parameter defined by $1 + \dfrac{\alpha_0 - \alpha_1}{\Delta}$
Z	coordinate normal to beam or column
Z	a column matrix
α	end rotational fixity parameter $= KL/EI$
β	end translational fixity parameter $= KL^3/EI$
Λ	a quantity defined by $\Lambda^2 = T$
Δ	$12 + 4(\alpha_0 + \alpha_1) + \alpha_0\alpha_1$
δ	lateral deflection of column
δ_{ij}	kronecker delta
η	w''
θ_i	slope in i^{th} buckle mode
λ	$\sqrt{PL^2/EI}$
φ_i	orthonormal function, $\theta_i(x)/\sqrt{N_i}$
ξ	location of concentrated lateral load
σ	a quantity defined by $(T + 2\Lambda)$

SUMMARY

For a very long time analysts and practicing engineers have been beset by uncertainty in defining the boundary conditions for real structures subject to destabilizing loads. Recently, some progress in the resolution of this question has been made. A new method of boundary evaluation, which associated the behavior of a structure under a non-destabilizing force system with the behavior of the same structure in a destabilizing environment, was proposed. The initial study demonstrated that in a number of cases the technique had significance for columns. However, the view point was restricted. It was not clear from the initial work whether the results were fortuitous or whether they were a consequence of a general principle. Empiricism, particularly when applied in a very specialized fashion can often yield results of interest for a particular or specific example and be value-less in any expanded problem. The question - how to determine the influence of realistic boundaries in a non-destructive fashion - is one of the most important. Thus, this thesis presents the results of detailed evaluations which clearly establish that the prior results are the outcome of a general relationship basic to the issue.

CHAPTER I

INTRODUCTION

It is generally accepted that the critical load for a relatively slender, geometrically perfect, centrally compressed column is given by the formula

$$P_{cr} = c \, \pi^2 EI / L^2 \qquad (1)$$

where c is the restraint coefficient, a quantity which characterizes the conditions of end fixity. Nevertheless, there is a major problem in the practical use of this simple equation. This difficulty was succinctly stated by Salmon [1] who wrote in 1921:

> The most pressing point for future research on the subject of columns is undoubtedly the question of the degree of imperfection in practical fixed ends; in short, what value of K[c]*should be assumed for such ends. A complete answer to this question is difficult, but, at present, the designer has no real data whatsoever regarding practical end conditions.

While a satisfactory answer to the above question remains to be found, the designer is not without some practical information pertaining to end restraint. Design conventions have emerged which are usually conservative and which can be applied with confidence to orthodox types of attachment. For example, Niles and Newell [2] present the following guidelines for airframe column members:

---

* K[c], end fixity coefficient.

As used in practice, the restraint coefficient is partly rational, partly empirical. A value less than 1.0 is seldom required, or a value greater than 2.0 permitted. Aeronautical engineers have customarily designed compression members in trusses having all-welded joints on the basis of c = 2.0, if the structure supporting the member was as stiff as, or stiffer than, the member itself. If the joints were made with several rivets or bolts, c was taken equal to 1.5 unless adequate test data were available to justify a larger coefficient. If the restraining effect of the contiguous structure was in doubt, c = 1.0 was used.

It is clear that these criteria are of questionable usefulness, especially in novel and innovative applications, and that more definitive information certainly is desirable for all cases.

Since Salmon's statement was made, much research on the subject of columns has been carried out. Great ingenuity has been expended by experimentalists in simulating the "ideal" end restraint conditions that are normally considered in analysis. A thorough review of these efforts has recently been prepared by Horton and Struble [3]. In this report the authors conclude that the complexity of achieving prescribed conditions and the fact that such conditions are rarely, if ever, met in actual structures provide strong justification for seeking a simple non-destructive testing method. A successful method of this type would yield data pertinent to the stability of column members with realistic end restraint without risk of costly damage or loss.

One powerful technique of column evaluation has already been established. This is the so-called Southwell Method. A review of its applicability to various types of structures is to be found in Reference [4]. Despite the power of this technique and its universal applic-ability in structural stability problems, it does not completely satisfy

the needs. The reason for this is that, before this method can be applied, data must be generated at destabilizing load levels which approach the critical. In this sense, the Southwell method can not be included in the category of the non-destructive test. It is perhaps more appropriately referred to as an indirect test.

Subsequent to the analysis of Southwell, Fisher [5] made a more detailed study. In this, he demonstrated that constant lateral load systems were effectively imperfections. Hence, lateral loading is a simple means of sensitizing columns to axial load effects. This means, then, that compressive load level can be reduced, data acquisition simplified and reliability enhanced by applying a constant lateral force. The Southwell critical load, being independent of imperfection level, is unaltered by the procedure.

Another approach to stability evaluation has been based upon relationships that exist between vibration frequencies and stability. It consists of measuring reductions in natural vibration frequencies as destabilizing load levels are increased. Stability limits may be estimated from vibration data obtained at subcritical values of load in this manner. This technique, as the Southwell method, is indirect rather than non-destructive in the sense explained earlier and does not appear to have received much attention [6].

Efforts [7,8,9,10] directed toward the development of truly non-destructive testing methods have recently been made. These center around the establishment of relationships between the behavior of the member under non-destabilizing conditions and in instability. The

approach adopted in References [7], [8], and [9] originated from the observation that buckling loads of columns are raised if end restraint stiffnesses are increased while the flexibility or compliance of the member under lateral loads is concomitantly decreased. These early investigations were concerned primarily with the establishment of empirical correspondence laws relating critical loads and compliances under lateral loads. The results obtained in this way are encouraging, but much additional work remains to be done.

A semi-analytical procedure is presented in Reference [10] which differs from the above. The author suggests applying lateral loads to the member, measuring parameters which vary with the end restraint stiffnesses and then inserting these measured values into stability equations in order to predict buckling. Obviously, this idea is both rational and straight-forward, but it does not permit measurements to be directly interpreted in terms of buckling. Moreover, since a precise theoretical calculation is required, extension of the method to more complex structural elements could present considerable difficulty.

To date the need for a practical non-destructive stability test is not yet satisfied. Nevertheless, by correlating buckling loads with compliances under lateral loads, progress has been made towards establishing such a test for columns. In the present work the background of this approach is reviewed in depth, a new correspondence law for columns is presented and a significant parameter associated with points of inflection identified. In addition, the practical application of the law is discussed and comparisons with previous laws are made.

CHAPTER II

NON-DESTRUCTIVE LATERAL LOAD TESTS

The work reported in References [7], [8], and [9] is basic to the current endeavor. The central idea presented in these pioneering efforts is perhaps best introduced by way of an illustration. Consider two similar columns of uniform bending stiffness with different conditions of end restraint - one simply supported and the other clamped at both ends. For these two configurations, the product of the respective buckling load and the maximum deflection caused by unit concentrated lateral force applied at the span mid-point is constant. That is

$$P_{cr} \left(\frac{\delta}{Q} \right) = \frac{\pi^2 L}{48} \tag{2}$$

where δ is the span mid-point deflection, Q is the magnitude of the concentrated lateral load, and L is the member length.

Equation (1) suggests that an increase (decrease) in restraint stiffness raises (lowers) P_{cr}, the buckling load of the beam acting as a column, and lowers (raises) the compliance (δ/Q) in such a way that the product of the two remains constant. Is this fact simply fortuitous or is it a consequence of a general principle of mechanics?

In an effort to answer this question, the remaining limiting cases of restraint were investigated [7]; the results are summarized in

Table 1. The best agreement corresponds to concentrated lateral loads applied so as to maximize the compliance (δ/Q). It is seen that equation (2) is adequate for all but the cantilever beam, in which case it gives results that are in error by a factor of four.

Struble [9] modified equation (2) to derive a rule which also applies to the cantilever. He noted that the difference between the cantilever and the other cases recorded in Table 1 is the number of inflection (zero moment) points that develop under both lateral and destabilizing forces. (The cantilever restraint produces a single inflection point, while the others result in two). Consequently, the modified law is of the form
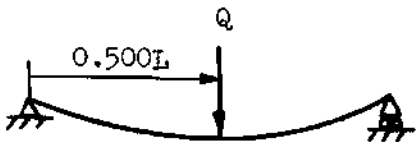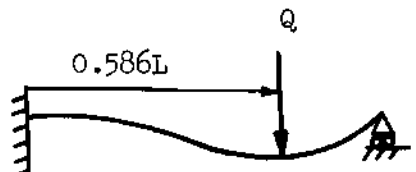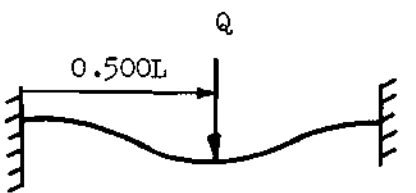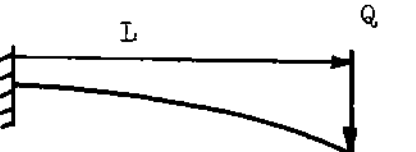
$$P_{cr}\left(\frac{\delta}{Q}\right) = \frac{\pi^2 L}{12n^2} \qquad (3)$$

where 'n' is the number of inflection points that develop within the span under the lateral loading. The incorporation of 'n' into the empirical law is similar to the introduction of the concept of effective or reduced length in the usual theory of column buckling; recall that a column's effective length is associated with the distance between inflection points in the buckled configuration.

Equation (3) can be appropriately called the load-deflection test. Following Struble [9], it will usually be abbreviated to simply "P-delta" test or law.

Results for beams of uniform bending stiffness or for limiting cases of restraint which correspond to either zero or infinite boundary

Table 1. Load-Deflection Test

Ideal Conditions of End Restraint	① $\dfrac{P_{cr} \cdot L^2}{\pi^2 \, EI}$	② $\dfrac{\delta_{max} \cdot EI}{Q \, L^3}$	① x 48 ② $48 \dfrac{P_{cr} \cdot \delta_{max}}{Q \pi^2 \, L}$
0.500L, Q	1.000	0.02083	1.000
0.586L, Q	2.045	0.00984	0.968
0.500L, Q	4.000	0.00521	1.000
L, Q	0.250	0.33333	4.000

restraint springs are not sufficient to substantiate the soundness of equation (3). Additional study [7,9] provided strong evidence that uniformity of bending stiffness is not essential for the P-delta law to remain valid. A systematic study [9] of the two elastically restrained configurations shown in Figures 1a and 1b was also conducted. For beams with elastic rotational restraint at the ends (Figure 1a), it was found that the maximum error incurred by using equation (2) is only 7 percent for all values of the rotational spring constants.

The P-delta test is no panacea, however. When applied to beams possessing the type of boundary restraint depicted in Figure 1b the agreement found is far from satisfactory in certain parameter ranges. A problem develops as the translational spring stiffness at the tip increases - the number of inflection points changes abruptly from one to two producing an unrealistic discontinuity in critical load prediction based upon equation (2). An error in P_{cr} of as much as 235 percent was reported by Struble [9] for this type of constraint; he then proposed an elaborate modification of the P-delta law in order to improve the situation, but the modified law was cumbersome to apply and the error remained unacceptably large for practical purposes.

An attendant experimental study [8] of the P-delta test was conducted using a test fixture designed to simulate the boundary conditions shown in Figure 1a. Maximum compliances were located by systematically varying lateral load positions along the beam specimens while critical loads were estimated by the Southwell method. Typical
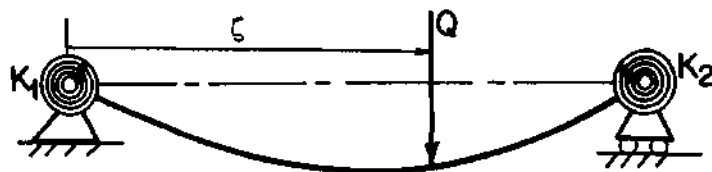
(a)

Unyielding Supports, Elastic Rotational Springs
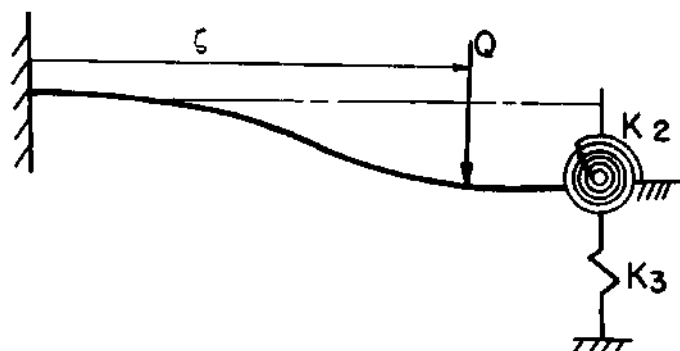
(b)

Cantilever with Elastically Supported Tip

Figure 1. Elastically Restrained Beam
Configuration

test results appear in Figure 2; it is evident that the product of the critical load and maximum compliance is constant.

While the value of the P-delta test cannot be denied, its shortcomings when lateral springs are present prompted a further search for a more comprehensive law. Noting that the transition from one to two inflection points was at the heart of the problem, Struble [9] made the following conjecture:

> We have thus far emphasized the importance of inflection points in beam behavior, indicating that there might be some sensitivity to wave form, as opposed to wave amplitude, that is lacking in the measurement of a single deflection only. It is noteworthy that an inflection point is also a point of extremal slope, and it is only natural to wonder if the measurement of maximum slopes might provide a better estimation of the buckling load than using the deflection approach.

He tenaciously employed a trial-and-error approach to finding laws relating the buckling loads and extreme values of slope or rotation.

Perhaps the most successful of the load-rotation or "P-theta" laws is

$$P_{cr}\left(\frac{\theta_m}{Q}\right) \cong \frac{\pi^2}{8} \tag{4}$$

where θ_m is the difference between the maximum and minimum values of the rotation angle produced by bending under the lateral load Q. The load is positioned so as to maximize θ_m. This relation is applicable without modification to the four limiting cases of restraint discussed
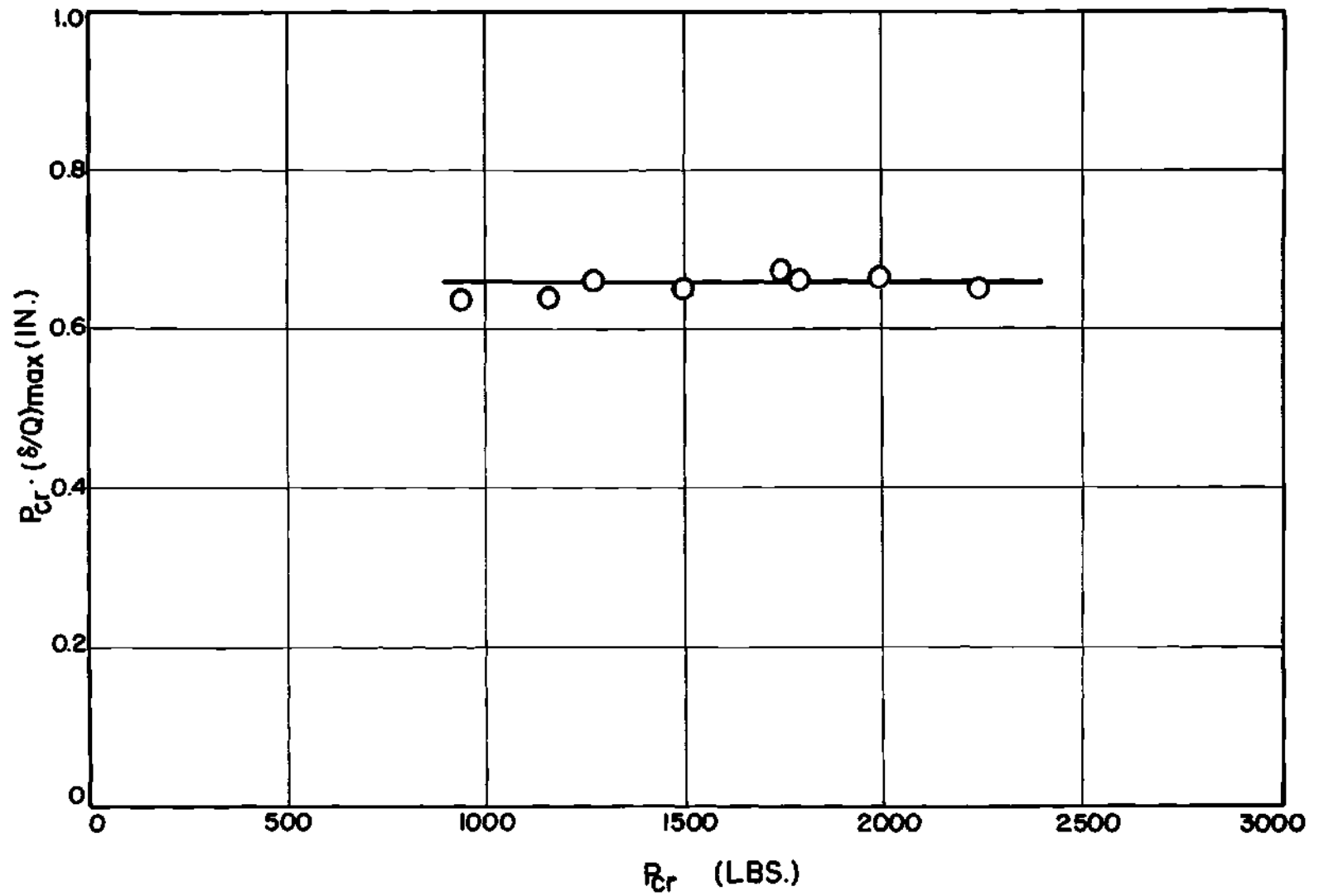
Figure 2. Typical Experimental Results of Horton and Ford (Reference 8).

earlier. It is illustrated in Table 2. It does not explicitly contain either material or geometric properties of the beam.
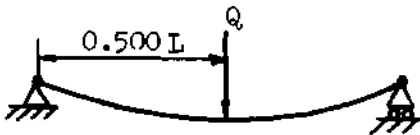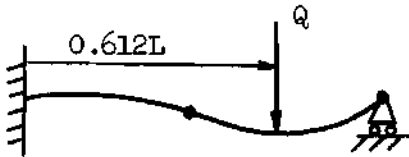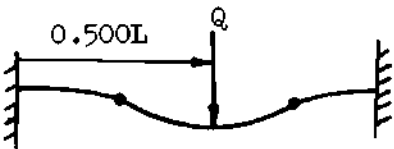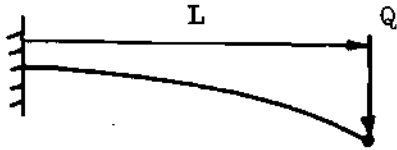
The adequacy of the P-theta test has been explored within the context of the elastically restrained configurations shown in Figures 1a and 1b. For beams on unyielding supports with ends elastically restrained against rotation (Figure 1a), the use of equation (4) results in a maximum error in critical load prediction of 6 percent for all values of end spring stiffnesses. Unfortunately, such good agreement cannot be achieved if a lateral spring is present (Figure 1b); unacceptably large errors in the range of weak lateral spring stiffness indicate that this test suffers from a deficiency comparable to that of the P-delta law.

In summary, it has been clearly established that both the P-delta and P-theta tests provide a sound basis for the evaluation of boundary effects for a wide class of structures subjected to destabilizing loads. These tests have been empirically developed, however. Their range of applicability is limited and their underlying principles have yet to be uncovered. Nevertheless, the potential usefulness of such methods is beyond question.

Introduction of a Uniformly Distributed Load

In the practical application of either the P-delta or P-theta tests, maximum flexibility locations are generally unknown at the outset. It becomes necessary, therefore, to search for them by applying lateral forces at a sufficient number of stations along the beam. Such a procedure produces a large quantity of data, of which

Table 2. Load-Slope Test.

Ideal Conditions of End Restraint	① $\dfrac{P_{cr} \cdot L^2}{\pi^2 EI}$	② $\dfrac{\theta_m \cdot EI}{Q L^2}$	① x 8 ② $8 \dfrac{P_{cr} \theta_m}{Q \pi^2}$
0.500 L, Q	1.000	0.1250	1.000
0.612L, Q	2.045	0.0609	0.996
0.500L, Q	4.000	0.0312	1.000
L, Q	0.250	0.5000	1.000

● Denotes inflection point.

only a fraction - the extreme values of compliance - are of any
interest if the P-delta or P-theta tests are used. In view of the
inadequacy of these two methods for weak lateral restraints and of the
quantity of unused data available, the question naturally arises
whether this data can be employed effectively to improve stability
predictions in the parameter ranges where improvement is needed.

We are strongly tempted to search for a meaningful statistic
such as some form of weighted average which incorporates all the data
obtained in traversing the beam. We are also cognizant that an
intimate relationship exists between a "moving" concentrated load and a
uniformly distributed load - the effects of the latter are the cumulative
or integrated effects of the former. At this point these two notions
coalesce to suggest a new direction - exploring the possibility of
relationships between a uniformly loaded beam and its stability limit.

We emphasize at the outset that uniformly distributed loading is
not recommended as practicable. It should be regarded as the convenient
limiting mathematical form for use in the search for empirical laws.
The recommended test procedure would consist of suitably superposing
data obtained from the application of a finite number of concentrated
loads along the beam span. We shall consider this matter in more
detail later in the discussion.

Search for Empirical Laws

The development of empirical laws is usually based upon an
intuitive step followed by inductive-deductive reasoning. In this the
experience gained in prior or similar situations is most helpful. So.

it has been in this study. Previous work indicated that extreme values of beam displacement and slope caused by lateral loads provide relevant compliance data. Moreover, the method of considering ideal limiting cases of end restraint first and then proceeding to more general situations has evolved as a pragmatic method of evaluating proposed empirical relations. These two notions serve to guide the course of our investigation.

We note that for a cantilever under uniform lateral load, q per unit length, the tip slope is given by

$$\theta = qL^3/6EI \tag{5}$$

and that the critical compressive load for an identical column under axial force is

$$P_{cr} = \pi^2 EI/4L^2 \tag{6}$$

whence it follows that

$$P_{cr} \cdot \theta = \frac{\pi^2 Lq}{24} \tag{7}$$

It should be noted at this juncture that the point at which the observation has been made is the tip of the beam. At this point there are certain other clearly definable conditions.

(1) the bending moment due to either the side load or the

axial load would be zero.

(2) the deflection in either load condition would be maximum.

(3) the slope at the tip can be regarded as a limiting case
since

$$\theta = \lim_{\Delta X \to 0} \frac{\delta_1 - \delta_2}{\Delta X}$$

where δ_1 is the lateral displacement determined at the tip and δ_2 is
the lateral displacement determined at a point Δx inboard of the tip.
It is also pertinent to note that

(4) the shear at the tip is zero.

(5) that the displacement curve under the action of the side
force has no inflection points.

The introduction of a sideways partial restraint at the tip
causes certain clear changes to take place. If the stiffness of the
restraining spring does not exceed a certain critical value then the
deflection at the tip will always be the maximum deflection in the beam
but when the value is exceeded it will no longer remain so. Moreover,
no matter how light the spring is, there will always be two zero
moment points along the beam, and there will always be a shear force
at the tip station.

We proceed now to examine the case of a simply supported beam.
Under a uniform load, q, the maximum slopes are located at the positions
of zero moment, viz. each end, and are given by

$$\theta = \frac{1}{24} \frac{qL^3}{EI} \tag{8}$$

The critical load level in this case is given by

$$P_{cr} = \frac{\pi^2 EI}{L^2} \tag{9}$$

and so

$$P_{cr} \cdot \theta = \frac{\pi^2 Lq}{24} \tag{10}$$

The similarity with the previous case is apparent. There is therefore a strong justification for examining the other limiting cases in the same fashion. At this stage certain complexities occur. We note now that if both of the beam ends are clamped, the positions of zero moment are no longer at the ends of the beam but are moved in from the ends by 0.211 L and are separated by a distance of 0.578 L. The slopes at these points are of course much reduced, having a value of

$$\frac{0.193}{24} \left(\frac{qL^3}{EI} \right).$$

It is apparent that the prior simple relationship is no longer applicable.

The discrepancy between the clamped-clamped and the other cases

can be simply resolved by a slight change in the comparison formula

used. We observe that the product

$$P_{cr} \, \theta max = 4 \times 0.193 \, \pi^2 \, \frac{qL}{24} = 0.772 \, \pi^2 \, \frac{qL}{24}$$
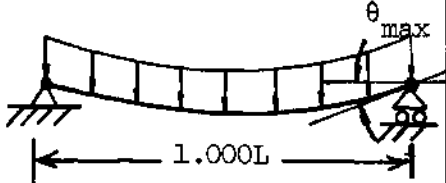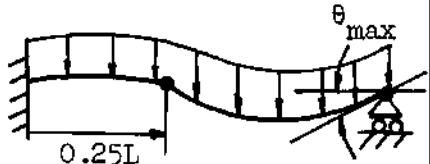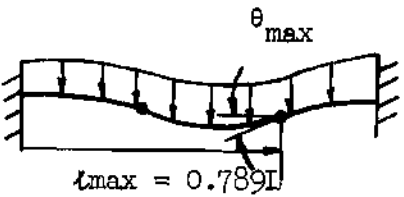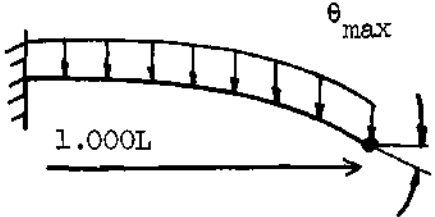
and that the θmax is positioned at a distance of 0.211 L or 0.789 L

from the end. Hence, we conjecture that a better quantity to consider

is the least value of $P_{cr} \, \theta max/\ell max$, where ℓmax is the greater of the

two distances from an end to the inflection point. Thus, we propose

the approximate relation

$$\frac{P_{cr} \, \theta max}{\ell max} \cong \frac{q\pi^2}{24} \tag{11}$$

The results obtained when this simple rule is used for the four ideal

cases are shown in Table 3. The buckling determinant and the equation

for beam slope under uniform lateral load for the rotationally

restrained body on unyielding lateral supports is derived in Appendix

A. From these derivations we can numerically evaluate the approximation

(11) in a broader context. The necessary computations were made on a

Univac 1108 and are summarized in Table 4. We see from this that

the expression is excellent for all combinations of end rotational

stiffness

A further examination of the case of a beam with one end clamped

and the other simply supported (propped cantilever) shows that the

Table 3. Distributed Load-Slope Test

Ideal Conditions of End Restraint	① $\dfrac{P_{cr}\,L^2}{\pi^2\,EI}$	② $\dfrac{24\,\theta_{max}\,EI}{l_{max}\cdot q\,L^3}$	① x ② $24\dfrac{P_{cr}\cdot\theta_{max}}{l_{max}\,q\,\pi^2}$
θ_{max} 1.000L	1.000	1.000	1.000
θ_{max} 0.25L	2.045	0.500	1.023
θ_{max} $l_{max} = 0.789L$	4.000	0.245	0.980
θ_{max} 1.000L	0.250	4.000	1.000

● Denotes inflecton point.

Table 4. Estimation of the Buckling Load by equation (11).

Stiffness Parameter α_0											
α_1	0	.5	1	2	5	10	50	100	10^3	10^5	
0	1.000	1.094	1.175	1.306	1.548	1.730	1.968	2.006	2.042	2.046	
	1.000	1.077	1.143	1.250	1.455	1.625	1.893	1.943	1.994	2.000	0
	0	-1.5	-2.7	-4.3	-6.0	-6.1	-3.8	-3.1	-2.3	-2.2	
.5		1.193	1.278	1.416	1.671	1.864	2.114	2.153	2.190	2.195	
		1.197	1.267	1.380	1.598	1.780	2.067	2.121	2.175	2.181	.5
		.3	-.9	-2.5	-4.3	-4.5	-3.3	-1.5	-.7	-.6	
1			1.367	1.512	1.780	1.982	2.243	2.284	2.323	2.327	
			1.372	1.492	1.721	1.914	2.217	2.275	2.332	2.339	1
			.3	-1.4	-3.3	-3.5	-1.2	-.4	.4	.5	
2				1.668	1.959	2.179	2.461	2.505	2.546	2.552	
				1.669	1.918	2.129	2.463	2.536	2.590	2.597	2
				0.0	-2.0	-2.3	.0	.8	1.7	1.9	
5					2.297	2.557	2.891	2.943	2.991	2.997	
					2.273	2.520	2.870	2.922	2.970	2.975	5
					-1.0	-1.5	-.7	-.7	-.7	-.7	
10						2.854	3.239	3.298	3.353	3.359	
						2.813	3.187	3.246	3.300	3.306	10
						-1.5	-1.6	-1.6	-1.6	-1.6	
50							3.700	3.711	3.838	3.845	
							3.718	3.789	3.855	3.863	50
							.5	.5	.4	.4	
100								3.845	3.914	3.921	
								3.896	3.965	3.973	100
								1.3	1.3	1.3	
10^3									3.984	3.992	
									4.077	4.085	10^3
									2.3	2.3	
10^5										4.000	
										4.098	10^5
										2.5	

Legend:
P_{cr} exact
P_{cr} estimated
% error

Stiffness Parameter α_1

relation (11) applies approximately if the slope value at the second inflection point is used. For this beam under the uniform load q, the slope at the inflection point remote from the pinned end is

$$\theta = 0.344 \frac{qL^3}{24EI}$$

and this point is located at a distance of 0.75 L from the pinned end. Thus,

$$\frac{P_{cr}\theta}{0.75L} = \left(\frac{0.344qL^3}{24EI}\right)\left(\frac{2.05\pi^2 EI}{L^2}\right)\left(\frac{1}{0.75L}\right) = 0.940\left(\frac{q\pi^2}{24}\right)$$

This observation suggests that equation (11) may be generalized. If we let θ_1 and θ_2 denote the two extreme values of slope that correspond to inflection points located at distances ℓ_1 and ℓ_2 from the remote ends of the beam (Figure 3), then we expect that

$$\frac{|\theta_1|}{\ell_1} \cong \frac{|\theta_2|}{\ell_2} \cong \frac{(|\theta_1| + |\theta_2|)}{(\ell_1 + \ell_2)}$$

Thus we can derive another equation as a replacement for equation (11).

$$\frac{P_{cr}(|\theta_1| + |\theta_2|)}{(\ell_1 + \ell_2)} = \frac{q\pi^2}{24} \tag{12}$$
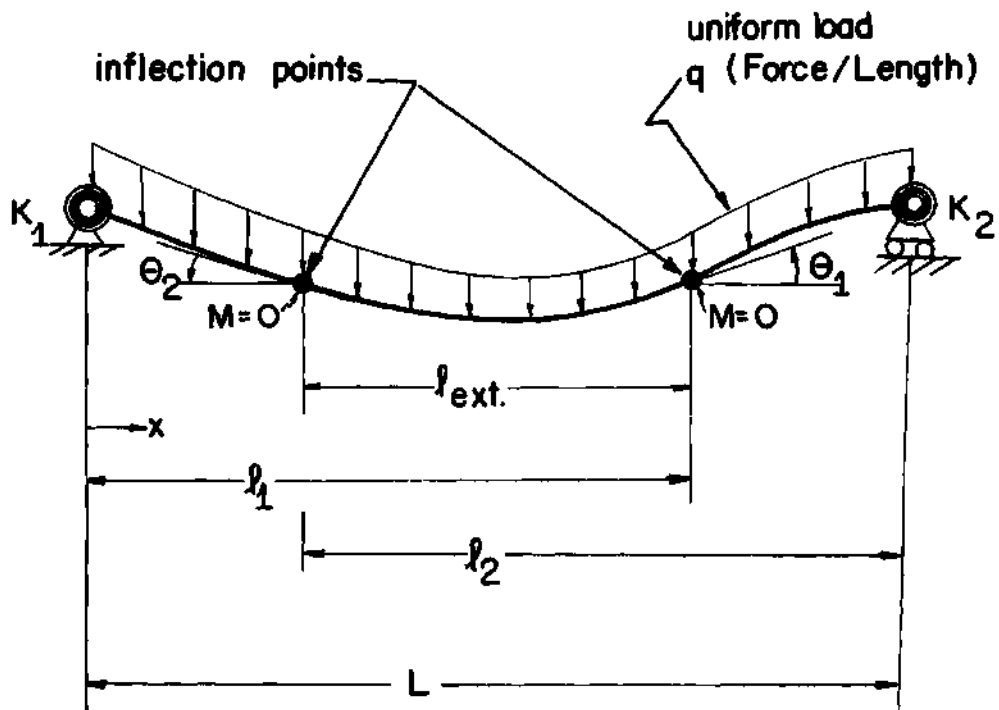
Figure 3. Geometric Parameters for an Elastically Restrained Beam.

where ℓ_1, ℓ_2, θ_1 and θ_2 are defined in Figure 3. In an effort to clarify the issue further the behavior of a beam with rotational end restraint at both ends is considered analytically (Appendix A). The lateral load is uniformly distributed and has a value of q per unit length. The analysis demonstrates that the sum of the absolute values of the slopes at the zero moment points is proportional to the cube of the distance apart of these points. This simple result has important practical consequences, because the formula (12) can now be written in the form

$$\frac{\left(\frac{P_{cr}}{EI}\right)(2 \cdot \ell_{ext}^3)}{(L + \ell_{ext})} = \pi^2 \tag{13}$$

In other words to evaluate the critical load under axial compression we do not need to measure slope at a point but merely distance apart of two points. Practically this is a much simpler operation.

The numerical calculations appropriate to this formula demonstrate that for all possible combinations of rotational spring stiffness the maximum error is only 2.5 percent. The results are shown in Table 5. The comparisons between the results by this test and those of "P-delta" and "P-theta" tests are shown in Figure 4.

The calculation was made for the case of equal rotational restraint, because for all three test methods this is the case in which the maximum error exists. It is seen that the result for the

Table 5. Errors Involved in the Estimation Formula equation (13).

			Stiffness Parameter α_0								
	0	.5	1	2	5	10	50	100	10^3	10^5	α_1
exact	1.000	1.094	1.175	1.306	1.548	1.730	1.968	2.006	2.042	2.046	
est.	1.000	1.095	1.176	1.303	1.535	1.715	1.977	2.023	2.069	2.074	0
%err	0.0	.1	.0	-.3	-.8	-.9	.4	.9	1.3	1.4	
		1.193	1.278	1.416	1.671	1.864	2.114	2.153	2.190	2.195	
		1.197	1.282	1.418	1.664	1.856	2.132	2.181	2.229	2.234	.5
		.3	.3	.1	-.5	-.5	.9	1.3	1.8	1.8	
			1.367	1.512	1.780	1.982	2.243	2.284	2.323	2.327	
			1.372	1.514	1.774	1.975	2.266	2.317	2.367	2.373	1
			.3	.2	-.3	-.3	1.0	1.4	1.9	2.0	
				1.668	1.959	2.179	2.461	2.505	2.547	2.552	
				1.669	1.950	2.169	2.484	2.539	2.593	2.600	2
				.0	-.5	-.5	.9	1.3	1.8	1.9	
					2.297	2.557	2.891	2.943	2.991	2.997	
					2.273	2.528	2.895	2.959	3.022	3.030	5
					-1.0	-1.2	.1	.5	1.0	1.1	
						2.854	3.239	3.298	3.353	3.359	
						2.813	3.227	3.300	3.371	3.380	10
						-1.5	-.4	.1	.5	.6	
							3.700	3.771	3.838	3.845	
							3.718	3.805	3.891	3.901	50
							.5	.9	1.4	1.5	
								3.914	3.924	3.921	
								3.896	3.985	3.995	100
								1.3	1.8	1.9	
									3.984	3.992	
									4.077	4.087	10^3
									2.3	2.4	
										4.000	
										4.098	10^5
										2.5	

Stiffness Parameter α_1

Legend: P_{cr} exact / P_{cr} estimated / % error

Figure 4. Comparative Results for Equal Rotational End Restraint

uniform load test is to all intents and purposes "exact".

Generalization to the Case of a Moving Lateral Support

In the arguments presented so far we have assumed that variation in rotational constraint is the prime problem of practical concern. We consider this to be a well founded assumption. Nevertheless, we realize that problems in which some flexibility exists in the lateral support system occur. The prior work [7,9] failed for these cases. The reason would appear to be that a single lumped compliance parameter cannot accomodate such complex boundary effects. Thus, a second parameter whose value is determined primarily by the lateral support flexibility must be introduced.

To search for this parameter we consider the elastically propped cantilever. To visualize the physics of the problem we begin with the plain cantilever beam. Under the action of a uniform lateral load this body deflects in a smooth curve and the maximum deflection and slope occur at the tip. The introduction of a partial sideways restraint at the tip causes certain clear changes to take place. If the stiffness of the spring does not exceed a certain critical value the deflection at the tip will always be the maximum for the beam. However, when this critical stiffness is exceeded this condition is no longer true. Moreover, no matter how light the spring is, there will always be two zero moment points along the beam, and the zero shear point will move away from the tip.

The propped cantilever for which the tip spring stiffness exceeds the critical value intuitively seems the easiest to deal with.

Thus, this case is treated first. It is readily apparent that the lateral spring can be replaced by an appropriate cantilever spring system. The requirements we must specify for this equivalent system are:

(1) The cantilever is to be regarded as a continuation of the beam under consideration. Therefore,

(a) it has the same EI as the beam

(b) it provides the same reaction force at the tip as does the real spring.

(c) there is continuity of slope and deflection at the proper point.

(2) To make the equivalent system handleable with the procedures previously followed the cantilever has an appropriate rotational spring at its root and an infinitely stiff lateral support.

With these conditions defined we may proceed to the analytical study of the problem. The system defined is depicted in Figure 5a and we note that at the tip there are initially four prescribed conditions viz known values of M_o, V_o, δ_o, θ_o. Two unknowns are to be ascertained from analysis - namely, the beam length and the end fixity coefficient α. It can be shown from the usual beam equations that the relationship between L and the prescribed conditions is

$$14 L^4 + 4V_o L^3 - 48M_o L^2 + 48\theta_o L - 48\delta_o = 0. \qquad (14)$$

The critical load for the configuration should be as follows:
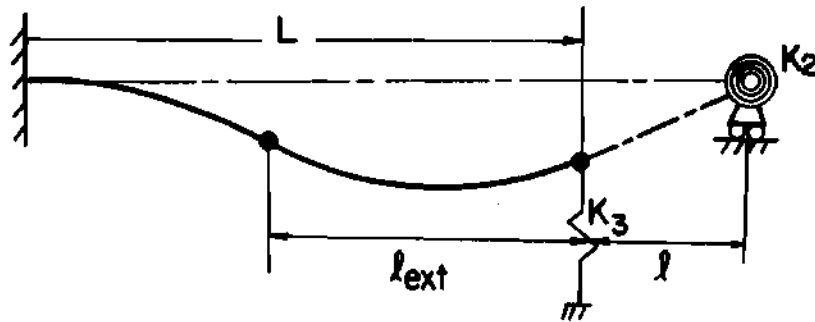
(a)

Analogy for Case I: $K_3 > 24 \dfrac{EI}{L^3}$
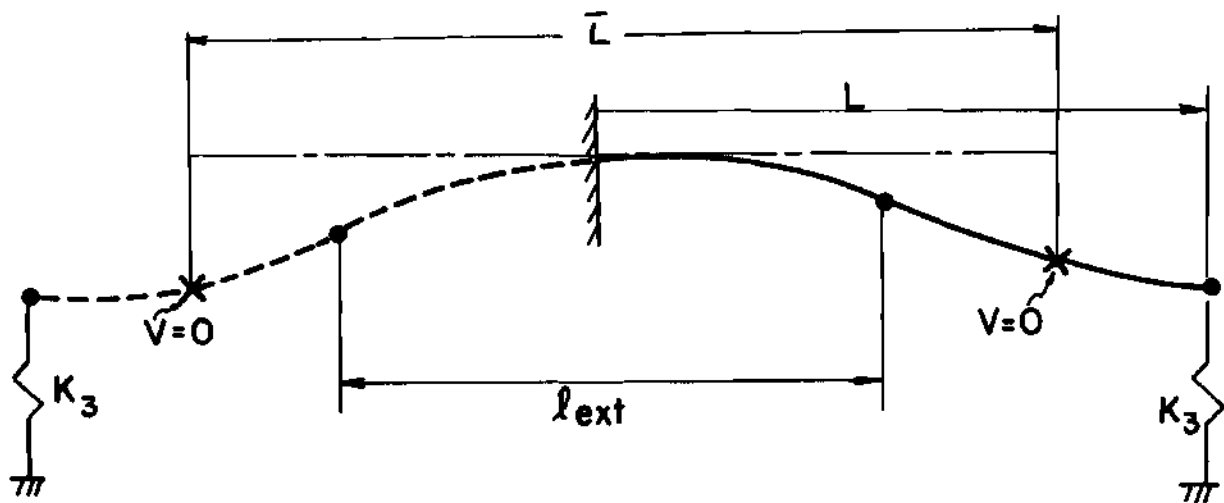
(b)

Analogy for Case II: $K_3 \leq 24 \dfrac{EI}{L^3}$

● Denotes Inflection Point

Figure 5. Beam Analogies for Cantilever with Lateral Tip Spring

$$P_{cr} = \frac{L + \ell_{ext}}{2\ell_{ext}^3} \cdot \frac{L^2}{(\ell + L)^2} \cdot \pi^2 EI \qquad (15)$$

where the term

$$\frac{L^2}{(L + \ell)^2}$$

is the natural correction for increase in column length from L to L + ℓ. This semi-empirical formula has been evaluated for values of

$$\frac{K_3 L^3}{EI}$$

ranging from the critical to virtual infinity. The error is acceptable over the whole spectrum. The extreme value, 13 percent, occurs at the lower bound. The average value is, however, much smaller as is clear from Table 6.

The cases for which the lateral support spring stiffness does not reach the value which causes the tip to be inclined upwards for a down loading of the beam cannot be treated by the procedure outlined. Thus, we are forced to a somewhat more intuitive approach. To deal with this case we go back to consider the relationship between the instability loads for a one-end clamped, one-end free column and a pin-pin column. We note immediately that the critical load of the first is given by

Table 6. Extended Beam Analogies.

Extended Beam Analogy Case (I)

$\dfrac{K_3 L^3}{EI}$	l	$\dfrac{P_{exact} \cdot L^2}{\pi^2 \, E \, I}$	$\dfrac{P_{est.} L^2}{\pi^2 \, E \, I}$	Errors (%)
24	.334	1.664	1.897	13
30	.302	1.731	1.766	3
40	.263	1.850	1.807	-3
100	.154	1.996	1.833	-8
500	.037	2.037	2.000	-1
	0	2.045	2.074	1

Extended Beam Analogy Case (II)

$\dfrac{K_3 L^3}{EI}$	$\dfrac{P_{exact} L^2}{\pi^2 \, E \, I}$	$\bar{L}$	l_{ext}	$\dfrac{P_{est.} L^2}{\pi^2 \, E \, I}$	Errors (%)
0	.250	2.0	2.0	.250	0
1	.332	1.8125	1.625	.328	-1.2
2	.414	1.7000	1.400	.407	-1.7
4	.572	1.571	1.142	.561	-1.9
8	.872	1.455	.910	.830	-4.8
16	1.360	1.368	.736	1.235	-9.2
24	1.664	1.333	.666	1.498	-10.0

$$P_{cr} = \frac{\pi^2 EI}{L_{cf}^2} \cdot \frac{1}{4} \qquad (16)$$

and the critical load for the second by

$$P_{cr} = \frac{\pi^2 EI}{L_{pp}^2} \qquad (17)$$

For equality of loads for these two systems we see immediately that

$$L_{pp} = 2L_{cf} \qquad (18)$$

And so, of course, we focus attention on the use of reflection in the study of the problem. But reflection of the beam to obtain an equivalent beam is not all that is necessary. Some parameter closely associated with the characteristics of the tip spring is essential. Instinctively we feel that this may well be the location of the point at which the shear is zero. We are given some confidence in this viewpoint by the fact that we can show this point to have significance in the case we have already treated.

Consider the beam column with uniform lateral loading and suppose that the zero shear point is positioned at distance L_1 from one end and L_2 from the other. Then we can demonstrate arithmetically that for a given beam

$$P_{cr} \times \left\{\frac{2\ell^3_{ext}}{2L_1 + \ell_{ext}}\right\} \left(\frac{2L_1}{L}\right) \simeq P_{cr} \times \left\{\frac{2\ell^3_{ext}}{2L_2 + \ell_{ext}}\right\} \left(\frac{2L_2}{L}\right) \simeq Constant \quad (19)$$

If we assume there are two functions ϵ_1 and ϵ_2 which make the above approximation identities, then we can write

$$P_{cr} \left\{\frac{2\ell^3_{ext} + \epsilon_1}{2L_1 + \ell_{ext}}\right\} \left(\frac{2L_1}{L}\right) = P_{cr} \left\{\frac{2\ell^3_{ext} + \epsilon_2}{2L_2 + \ell_{ext}}\right\} \left(\frac{2L_2}{L}\right) \qquad (13)$$
<div align="right">bis</div>

$$= P_{cr} \left\{\frac{4(L_1 + L_2)\,\ell^3_{ext} + 2L_1\epsilon_1 + 2L_2\epsilon_2}{2(L_1 + L_2) + 2\ell_{ext}}\right\}\left(\frac{1}{L}\right)$$

$$= P_{cr} \left\{\frac{2\ell^3_{ext}}{L + \ell_{ext}}\right\} + \epsilon = Constant$$

In essence, when ϵ is regarded as the error, this is the formula previously derived. Hence, we see that the zero shear point is an important point on the beam but we note that in the previous investigations this fact was masked.

We proceed now to reexamine the question of the subcritical propped beam. We begin by reflecting the beam and considering the equivalent length to be the distance between the zero shear points. This, of course, differs from the true length and thus we anticipate some correction will be required. As before, the natural correction should be the ratio of the squares of the equivalent and real lengths. With these ideas in mind the analogous expression should be

$$\left(\frac{P_{cr}}{EI}\right) \frac{2\ell^3_{ext}}{L + \ell_{ext}} \left(\frac{L}{2L}\right)^2 = \pi^2 \tag{20}$$

This semi-empirical formula turns out to be a very good approximation, the maximum error being of the order of 10 percent. The values of the theoretically exact and approximate P_{cr}'s together with the appropriate errors are shown in Table 6.

Now it has become clear that the characteristic distance between inflection points under a uniformly distributed lateral force is an important parameter in the mathematical description of the influence of boundaries on instability load of columns. So, at this stage it is worthwhile examining the predecessor's work, i.e., "P-delta" and "P-theta" methods, to find out whether they can be associated with the same quantity. To clarify this point the deflection, slope and moment due to a concentrated lateral force acting on an end rotationally restrained beam with unyielding lateral supports was derived. The derivation is given in section (c) of Appendix A. The analysis shows that when the rotational restraints are equal, the sum of the absolute values of the extremum slopes, which was used as a parameter in "P-theta" method is proportional to the square of the distance between the inflection points. Therefore, in this case, the "P-theta" method is equivalent to the following relation

$$\left(\frac{P_{cr}}{EI}\right) \cdot \ell^2_{ext} = \frac{\pi^2}{2} \tag{21}$$

where ℓ_{ext} is the distance between the two inflection points when a concentrated lateral force is applied at the mid-span of the column considered.

Non-Uniform Cross Section

So far in the analysis the bending stiffness of the column has been assumed to be uniform. Now the question is "Is the uniformity of the bending stiffness essential to the issue presented here?" With regard to this question, Reference [7] showed one example of the variable bending stiffness problem for the clamped-pinned boundary condition and proved the applicability of the so-called "P-delta" method. In this thesis a simple empirical formula relating the buckling load of the column of variable bending stiffness to the extremum slopes due to a uniformly distributed lateral force is investigated extensively. As a first example, the simply supported strut depicted in Figure 6 is considered. This strut is non-uniform, the two halves having different bending stiffness. According to J. Case [11] the critical load for a strut unsymmetrical about the center is given by

$$\frac{2}{P_{cr}} = \frac{1}{P_a} + \frac{1}{P_b} \tag{22}$$

where P_a is the buckling load of a strut with two halves like OA, and P_b is the buckling load of a strut with two halves like OB. Since the
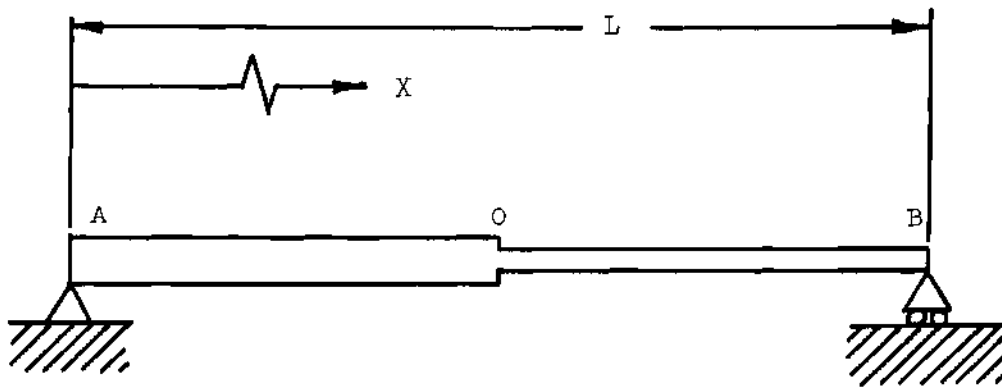
Figure 6. Non-Uniform Beam Unsymmetric About its Center.

inflection points are always at the ends for this configuration, and the signs of the slopes at the two ends are opposite, the sum of the absolute values of the extremum slopes is their algebraic difference. When the uniformly distributed lateral force of intensity q (lb/in) is applied to the column considered, the governing differential equations are

$$EI_1 W'' = \frac{qL}{2} X - \frac{q}{2} X^2 \qquad 0 \leq X \leq \frac{L}{2} \qquad (23)$$

$$EI_2 W'' = \frac{qL^2}{8} - \frac{q}{2} (X - \frac{L}{2})^2 \qquad \frac{L}{2} \leq X \leq L$$

Integrating both equations in (23) yields

$$EI_1 W' = \frac{qL}{4} X^2 - \frac{q}{6} X^3 + C_1 \qquad 0 \leq X \leq \frac{L}{2} \qquad (24)$$

$$EI_2 W' = \frac{qL^2}{8} X - \frac{q}{6}(X - \frac{L}{2})^3 + C_2 \qquad \frac{L}{2} \leq X \leq L$$

The condition of slope continuity at $X = L/2$ gives

$$\left(\frac{C_2}{I_2} - \frac{C_1}{I_1}\right) = qL^3 \left\{ - \frac{1}{16}\left(\frac{1}{I_2}\right) + \frac{1}{24}\left(\frac{1}{I_1}\right)\right\} \qquad (25)$$

Hence

$$E\left(w'_{X=L} - w'_{X=0}\right) = \frac{qL^3}{24}\left(\frac{1}{I_1} + \frac{1}{I_2}\right) \tag{26}$$

Equation (22) can be re-written as

$$P_{cr} = \frac{\pi^2 E}{L^2} \frac{2}{\left(\frac{1}{I_1} + \frac{1}{I_2}\right)} \tag{27}$$

and this in conjunction with equation (26) becomes

$$P_{cr} \cdot \Delta\theta = \frac{\pi^2 Lq}{12} \tag{28}$$

Now equation (28) can be re-written as

$$\frac{P_{cr} \cdot \Delta\theta}{2L} = \frac{\pi^2 q}{24} \tag{29}$$

which is, of course, equation (12) precisely.

The second case considered is the clamped-pinned column as depicted in Figure 7. The bending stiffness, in general, can be written as

$$EI(x) = EI_0\left\{1 - \frac{1}{T}\left(\frac{X}{L}\right)^p\right\} \tag{30}$$

q=constant

X= 0   X= L
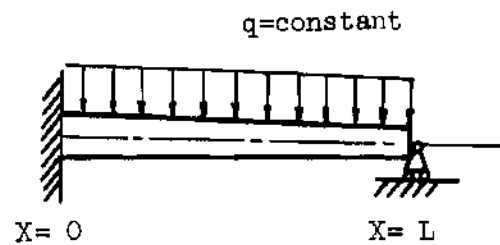
Figure 7.   Clamped-Pinned Beam of Variable Bending Stiffness

under the Uniformly Distributed Load

q=constant

X=0   X=L
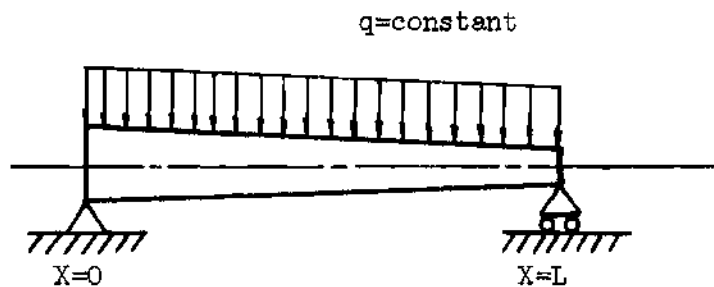
Figure 8.   Simply Supported Beam of Variable Bending Stiffness

under the Uniformly Distributed Load

where T, a number greater than 1, represents the taper ratio of the bending stiffness and EI_o is the bending stiffness at the root.

The slope at the pinned end, which is of prime interest here, due to a uniform lateral force is obtained by integrating the differential equation

$$\frac{\partial^2}{\partial X^2}\left\{EI(X)W''\right\} - q = 0 \tag{31}$$

and staisfying the boundary conditions

$$W = W' = 0 \quad \text{at} \quad X = 0 \tag{32}$$

$$W = W'' = 0 \quad \text{at} \quad X = L$$

The slope as a function of T was calculated for the p = 1 and p = 2 cases. The details are given in Appendix D. The buckling load was calculated by the finite difference method [12] using Potter's [13] method and its modification [14]. The set up of the finite difference equation, the computer program in Fortran language, and the numerical results for p = 1 and p = 2 cases are also shown in Appendix . The buckling loads, ratios, the tip slope parameters and the products of the two quantities are listed in Tables 7 and 8, for different values of T. The results clearly confirm the excellent accuracy of the empirical law (11), viz.

Table 7. Propped Cantilever Beam with Linearly Varying Bending Stiffness

(1)	(2) Buckling Load Ratio	(3) Tip Slope Parameter	(4)	(5)
T	$\dfrac{P_{cr}L^3}{\pi^2 EI}$	$\dfrac{24\theta_{end}}{\dfrac{qL^3}{EI_o}}$	Product (2)x(3)	Error (%) in Equation (11)
1.053	.810	1.466	1.187	18.7
1.071	.846	1.387	1.173	17.3
1.111	.914	1.259	1.151	15.0
1.125	.934	1.224	1.143	14.3
1.250	1.085	1.023	1.110	11.1
1.500	1.277	.846	1.080	8.0
1.750	1.430	.760	1.087	6.7
2	1.492	.710	1.059	5.9
3	1.687	.618	1.043	4.3
5	1.834	.563	1.033	3.2
10	1.940	.514	0.997	-.3
20	1.993	.508	1.012	.6
100	2.034	.503	1.023	1.1

Table 8. Propped Cantilever with Parabolically
Varying Bending Stiffness

(1)	(2) Buckling Load Ratio	(3) Tip Slope Parameter	(4)	(5)
T	$\dfrac{P_{cr} \cdot L^2}{\pi^2 EI}$	$\dfrac{24\theta_{end}}{\dfrac{qL^3}{EI_o}}$	Product (2) x (3)	Error (%)
1.053	1.182	1.035	1.223	22.4
1.071	1.208	1.001	1.204	20.9
1.111	1.258	.942	1.185	18.5
1.125	1.274	.926	1.180	17.9
1.143	1.293	.906	1.171	17.2
1.167	1.316	.884	1.163	16.3
1.250	1.384	.824	1.140	14.0
1.750	1.606	.674	1.082	8.2
2	1.673	.643	1.074	7.4
3	1.808	.583	1.054	5.3
5	1.907	.545	1.039	3.9
10	1.974	.521	1.028	2.8
20	2.011	.510	1.026	2.5
100	2.035	.505	1.028	1.4

$$P_{cr} \cdot \left(\frac{\theta_{ext}}{L}\right) = \frac{\pi^2 q}{24} \qquad\qquad \text{(11)}$$

<div align="right">bis</div>

The maximum deviation of the product of the critical load and slope parameter differs from the constant

$$\left(\frac{\pi^2 q}{24}\right)$$

by only a few percent for all practically realistic values of T.

The third case considered is that of the simply supported beam, (Figure 8). The bending stiffness is assumed from the form given in equation (30). Linear (p=1) and Parabolic (p=2) cases are considered for different values of T. The extremum slopes are located at the ends and are of different signs. Thus, the sum of the absolute values of the extremum slopes is the difference of the end slopes which are calculated in Appendix . As before, the buckling load was obtained by a finite difference scheme. The appropriate computer program is given in Appendix . The only deviation from the clamped-pinned case lies in the boundary matrix corresponding to the left end. The empirical law

$$P_{cr}\left\{\frac{|\theta_1| + |\theta_2|}{2L}\right\} = \frac{q\pi^2}{24}$$

was checked for this configuration. The values of critical load and the slope parameters and the product of the two are listed in Table 9 and 10 for different values of T. It is readily seen from these tables

Table 9. Simply Supported Beam with Linearly Varying
Bending Stiffness

(1)	(2) Buckling Load Ratio	(3) Tip Slope Parameter	(4)	(5)
T	$\dfrac{P_{cr}L^2}{\pi^2 EI}$	$\dfrac{12\ \Delta\theta}{\dfrac{qL^3}{EI_o}}$	Product (2)x(3)	Error (%) in Equation (11)
1.053	.429	2.440	1.047	4.7
1.071	.442	2.343	1.036	3.6
1.111	.472	2.179	1.028	2.8
1.125	.482	2.133	1.028	2.8
1.143	.493	2.080	1.025	2.5
1.250	.548	1.853	1.015	1.5
1.500	.636	1.584	1.007	.7
1.750	.690	1.448	0.999	-.1
2	.734	1.364	1.001	.1
3	.827	1.210	1.001	.1
5	.897	1.114	0.999	-.1
10	.949	1.053	0.999	-.1
20	.974	1.025	0.998	-.1
100	.995	1.005	1.000	-.0

Table 10. Simply Supported Beam with Parabolically
Varying Bending Stiffness.

(1)	(2) Buckling Load Ratio	(3) Tip Slope Parameter	(4)	(5)
T	$\dfrac{P_{cr}L^2}{\pi^2 EI}$	$\dfrac{12\Delta\theta}{\dfrac{qL^3}{EI_0}}$	Product (2)x(3)	Error (%) in Equation (11)
1.053	.641	1.660	1.064	6.4
1.071	.651	1.625	1.058	5.8
1.111	.672	1.563	1.050	5.0
1.125	.678	1.545	1.048	4.8
1.143	.687	1.524	1.047	4.7
1.250	.725	1.430	1.037	3.7
1.500	.782	1.309	1.024	2.4
1.750	.818	1.244	1.018	1.8
2	.844	1.201	1.014	1.4
3	.900	1.120	1.008	.7
5	.941	1.066	1.033	.3
10	.971	1.032	1.032	.2
20	.985	1.015	1.000	.0
100	.997	1.003	1.000	.0

that the formula (11) is an excellent approximation. The excellence
of the formula (11) for a uniformly distributed load cannot be denied,
but its practicality can readily be challenged. The characteristics
of a uniformly distributed load are relatively simple to analyze but
relatively difficult to achieve in the laboratory. Admittedly a
uniform load can be regarded as the integrated effect of a series
of discrete loads or as that of a moving load but this clearly
presents practical difficulties. In short, uniformity is a wonderful
mathematical expedient but a poor laboratory tool. Thus, the next
step in making the work fully practical must be to ascertain whether
the uniform load can be replaced by a discrete load system without
inducing unacceptable errors. A detailed analysis of this question has
been made for the beam on unyielding supports. It shows that three
equal forces applied at the 1/4, 1/2 and 3/4 points of the beam can
be used to determine the characteristic length with reasonable
accuracy. The errors involved in this determination are depicted in
Table 11 while the effects of other multiple discrete load systems are
portrayed in Figures 9 through 14. The use of a three force system
simplifies the question of load application, just as characteristic
length used in the analysis improved the ease of determination of the
necessary length parameter.

Table 11. Estimation of the Buckling Load by Applying Three Equally
Spaced Concentrated Lateral Forces on the Rotationally
Restrained Beam

	Stiffness Parameter (KL/EI)										
	0	.5	1	2	5	10	50	100	10^3	10^5	
	1.000	1.094	1.175	1.306	1.548	1.730	1.968	2.006	2.042	2.046	
	1.000	1.116	1.208	1.345	1.568	1.723	1.837	1.924	1.957	1.985	0
	0.0	2.0	2.8	3.6	1.3	-.4	-6.7	-4.1	-4.2	-3.0	
		1.193	1.278	1.416	1.671	1.864	2.114	2.153	2.190	2.195	
		1.244	1.347	1.499	1.746	1.916	2.132	2.167	2.201	2.204	.5
		4.3	5.4	4.5	2.8	.9	.7	.5	.5	.4	
			1.367	1.512	1.780	1.982	2.243	2.284	2.323	2.327	
			1.457	1.622	1.889	2.072	2.302	2.340	2.375	2.379	1
			6.6	7.3	6.1	4.5	2.6	2.5	2.2	2.2	
				1.668	1.959	2.179	2.461	2.505	2.546	2.552	
				1.806	2.104	2.308	2.563	2.604	2.643	2.647	2
				8.3	7.4	5.9	4.1	4.0	3.8	3.7	
					2.297	2.557	2.891	2.943	2.991	2.997	
					2.4 6	2.699	3.003	3.051	3.097	3.102	5
					6.9	5.6	3.9	3.7	3.5	3.5	
						2.854	3.239	3.298	3.353	3.359	
						2.971	3.314	3.369	3.421	3.427	10
						4.1	2.3	2.2	2.0	2.0	
							3.700	3.711	3.838	3.845	
							3.714	3.779	3.840	3.847	50
							.4	1.8	5.2	.1	
								3.845	3.914	3.921	
								3.845	3.908	3.916	100
								0.0	-.2	-.1	
									3.984	3.992	
									3.973	3.981	10^3
									-.3	-.3	
										4.000	
										3.988	10^5
										-.3	

Legend box:

P_{cr} exact
P_{cr} estimated
% error

(right axis label: Stiffness Parameter (KL/EI))

Figure 9. Multiple Concentrated Lateral Loads Tests -- $\alpha_o = 0$ case
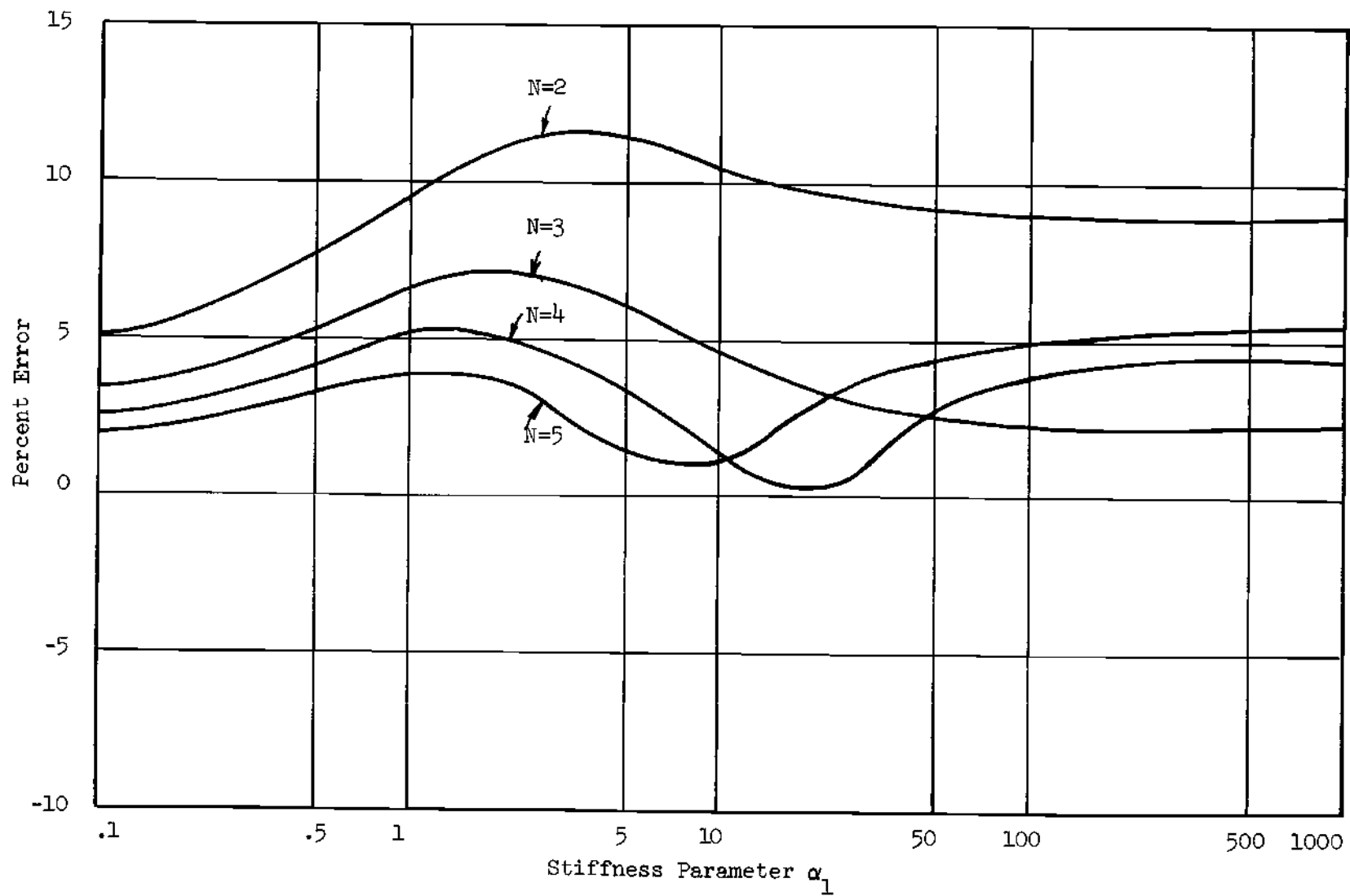
Figure 10. Multiple Concentrated Lateral Load Tests -- $\alpha_o = 1$ case
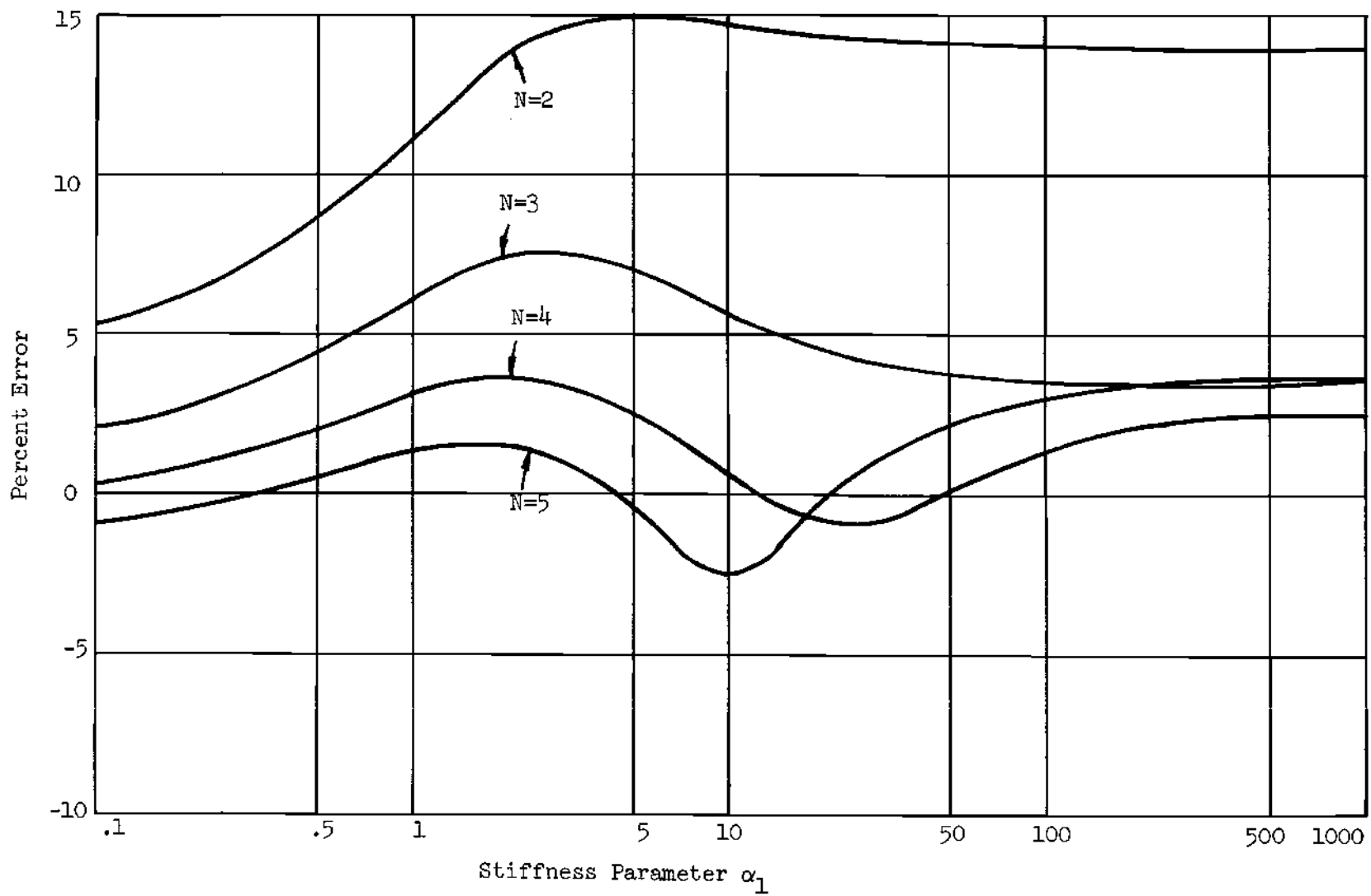
Figure 11. Multiple Concentrated Lateral Loads Tests -- $\alpha_o = 5$ case
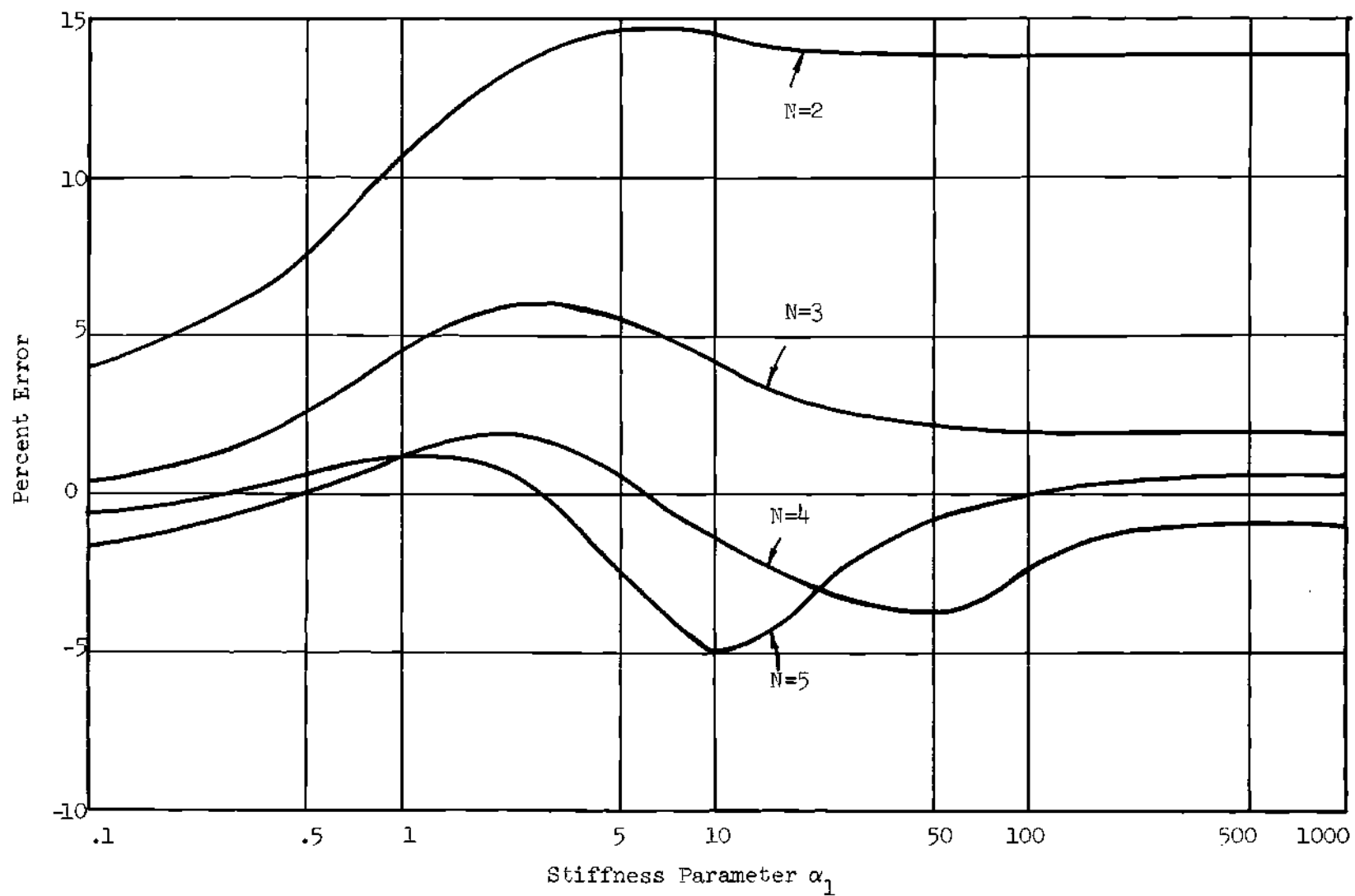
Figure 12. Multiple Concentrated Lateral Loads Test -- α_o = 10 case
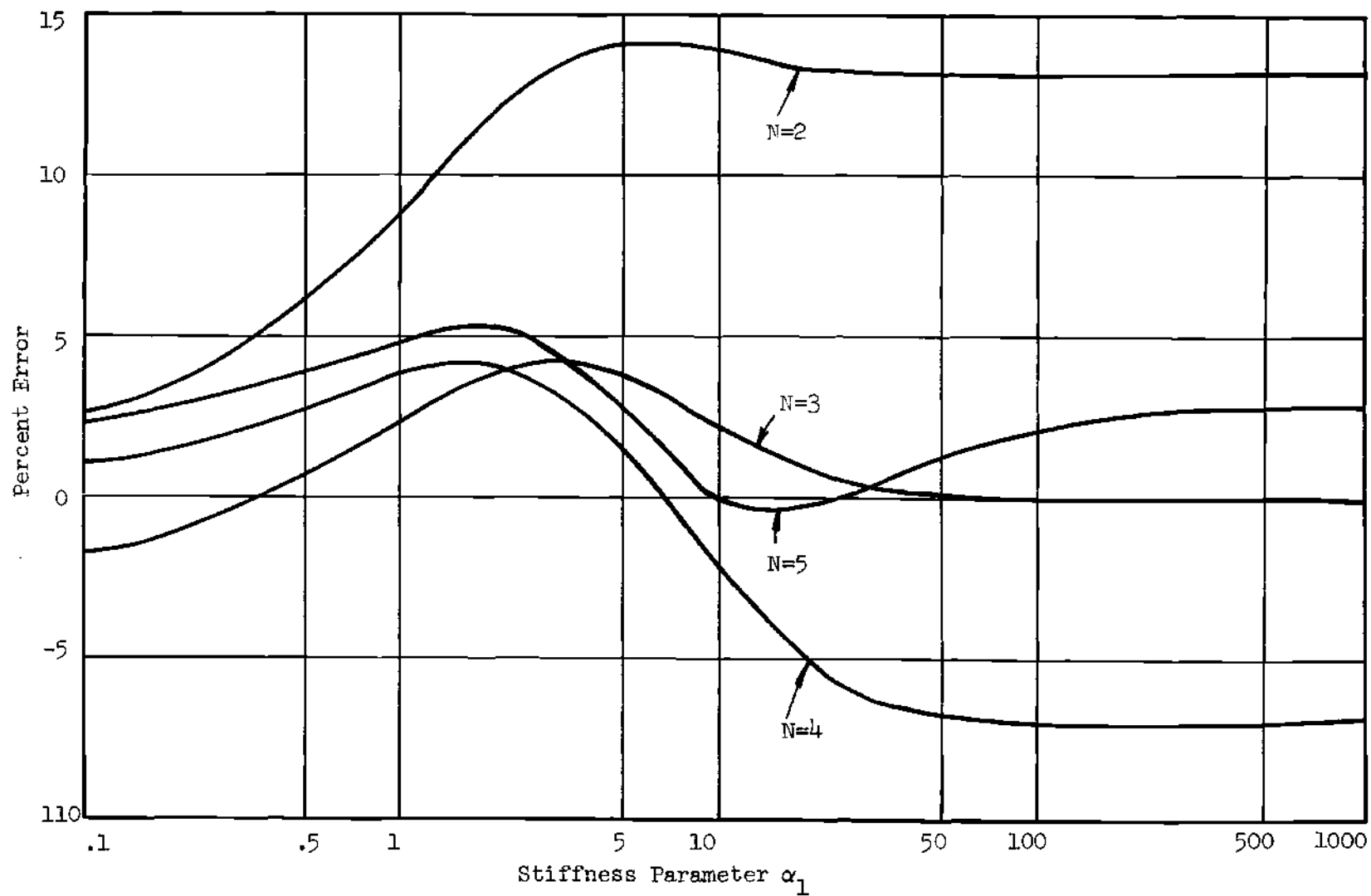
Figure 13. Multiple Concentrated Loads Test -- $\alpha_o = 100$ case
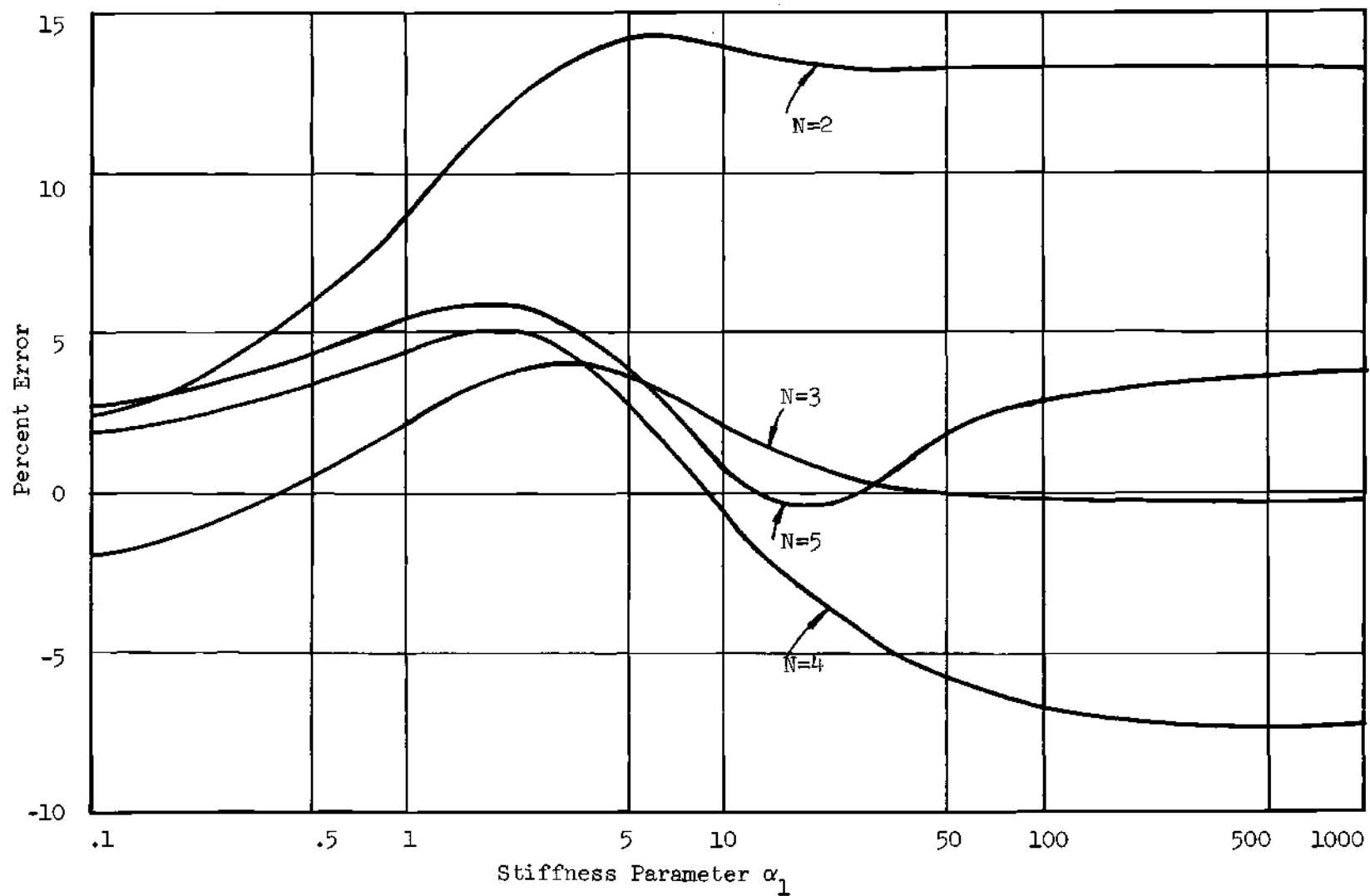
Figure 14. Multiple Concentrated Lateral Loads Test -- $\alpha_o = 1000$ case

CHAPTER III

GENERAL INTEGRAL EQUATION FORMULATION

Formulation of the Integral Equation

The work in the preceding sections as well as that in reference [9] has given very clear indication that the instability behavior of a partially restrained column can be readily associated with the deformations of the same body under lateral load. We are led, therefore, to the thought that a clearer understanding of the relationships established might be derived from an analysis of the beam column. To this end an integral equation approach to stability load level determination is developed in this chapter.

In formulating the integral equation for column buckling, it is convenient to introduce the idea of equivalent buckling force. Consider the elastically supported beam as beam-column shown in Figure 15.

The work done by the axial force P, is

$$W_e = P \; \tfrac{1}{2} \int_o^L (W')^2 \; dX \tag{41}$$

The virtual work of the axial load is
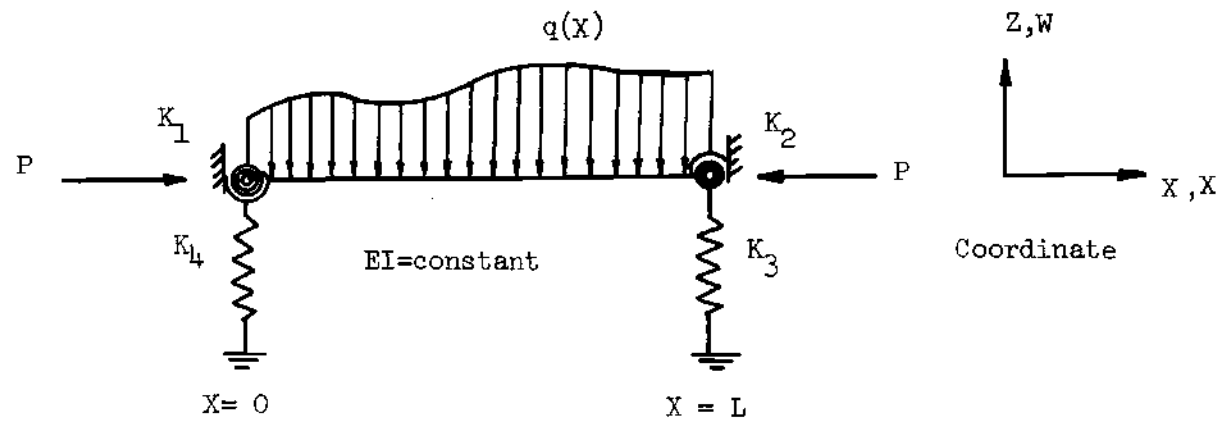
Figure 15 . Elastically Supported Beam Under Combined Loading.

$$\delta W_e = P \int_0^L W'\delta W' dX = PW'\delta W \Big|_0^L - P \int_0^L W''\delta W dX \qquad (42)$$

Interpretation of equation (42) becomes clear when the variation of the external potential is written for a beam under a load distribution $q(X)$ and shear forces $S(0)$ and $S(L)$ on the boundaries. That is

$$\delta W_e = S(X) \delta W \Big|_0^L + \int_0^L q(X) \delta W dX \qquad (43)$$

Comparison of equation (42) with equation (43) shows that in this problem there are equivalent force systems. The system with which we begin can be replaced by the distributed moment $-PW''$ upwards and additional boundary shear forces, $PW'(L)$ upward at $X = L$ and $PW'(0)$ downward at $X = 0$.

Thus the effective distributed load q_{eff} acting upward is defined as

$$q_{eff} = -PW''(X') - PW'(X')\delta(X') + PW'(X')\delta(X'-L) \qquad (44)$$

$$= -P[W''(X') + W'(X')\delta(X') - W'(X')\delta(X'-L)]$$

where $\delta(X')$ is a Dirac delta function.

In general when the loading $q(X)$ is distributed over the beam, the deflection at X, $W(X)$, can be written

$$W(X) = \int_{0}^{L} C(X,X')q(X')dX' \tag{45}$$

where $C(X,X')$ is the flexibility influence function interpreted as the displacement at X due to a unit lateral force at X'.

For the sake of simplicity in the analysis which follows, non-dimensional quantities defined below are introduced.

$$x = \frac{X}{L} , \quad \zeta = \frac{X'}{L} , \quad w = \frac{W}{L} , \quad \bar{P} = \frac{PL^2}{EI}$$

$$\bar{q}(\zeta) = \frac{qL^3}{EI} , \quad \bar{C}(x,\zeta) = \frac{C(X,X')}{L}$$

Equation (44) and (45) can now be rewritten as follows:

$$\bar{q}_{eff} = -\bar{P}[w''(\zeta) + w'(\zeta)\delta(\zeta) - w'(\zeta)\delta(\zeta-1)] \tag{46}$$

$$w(x) = \int_{0}^{1} \bar{C}(x,\zeta)\bar{q}(\zeta)d\zeta \tag{47}$$

Replacing $\bar{q}(\zeta)$ in equation (47) by $\bar{q}_{eff}$, the following relation is obtained.

$$w(x) = \int_0^1 \bar{C}(x,\zeta)\bar{q}_{eff}(\zeta)d\zeta \qquad (48)$$

$$= -\bar{P}\int_0^1 \bar{C}(x,\zeta)[w''(\zeta) + w'(\zeta)\delta(\zeta) - w'(\zeta)\delta(\zeta-1)]d\zeta$$

$$= -\bar{P}\int_0^1 \bar{C}(x,\zeta)w''(\zeta)d\zeta - \bar{P}\bar{C}(x,0)w'(0) + \bar{P}\bar{C}(x,1)w'(1)$$

Integration of the first term in equation (48) by parts yields terms which cancel boundary terms, and when this is done the resulting equation is,

$$w(x) = \bar{P}\int_0^1 \frac{\partial \bar{C}(x,\zeta)}{\partial \zeta} w'(\zeta)d\zeta \qquad (49)$$

It is convenient for some application to write the previous equation in terms of the slope. Taking the derivative of equation (49) with respect to x, an alternative form of this equation is obtained.

$$w'(x) = \bar{P}\int_0^1 \frac{\partial^2 \bar{C}(x,\zeta)}{\partial x \partial \zeta} w'(\zeta)d\zeta \qquad (50)$$

Since no specific restriction on the boundary conditions was imposed in deriving equations (49) and (50), these two equations are valid for all boundary conditions. Here, for the sake of convenience, the following notations are introduced.

$$r(x,\zeta) = \frac{\partial^2 \bar{C}(x,\zeta)}{\partial x \partial \zeta} \qquad (51)$$

$$\theta(x) = w'(x)$$

$$d(x,\zeta) = \frac{\partial \bar{C}(x,\zeta)}{\partial \zeta}$$

where $r(x,\zeta)$ and $d(x,\zeta)$ are interpreted as the slope and deflection, respectively, due to a unit moment applied at the location ζ. It should also be noted that $r(x,\zeta)$ is symmetric with respect to x and ζ, as can be shown from the reciprocal theorem.

Using these notations, equations (49) and (50) can now be written as follows:

$$w(x) = \bar{P} \int_0^1 d(x,\zeta)\theta(\zeta)d\zeta \qquad (52)$$

$$\theta(x) = \bar{P} \int_0^1 r(x,\zeta)\theta(\zeta)d\zeta \qquad (53)$$

Orthogonality Relations

For the ideal boundary conditions, namely, simply supported, built-in or free, the following orthogonality relations are known to be true [15].

$$\int_0^1 W'_n W'_m \, dX = 0 \tag{54}$$

and

$$\int_0^L EI(X) W''_m W''_n \, dX = 0 \tag{55}$$

where W_m and W_n are the mth and nth buckling mode associated with the buckling load P_m and P_n respectively. Equation (54) is, of course, a general result. The detail of the derivation is given in Appendix A. The orthogonality relation (equation (10)) in Appendix B can be rewritten as follows:

$$\int_0^1 \theta_i(x) \theta_j(x) \, dx = N_i \delta_{ij} \tag{56}$$

where

$$N_i = \int_0^1 \theta^2_i(x) \, dx$$

$$\delta_{ij} = \text{Kronecker delta}$$
$$\left(\begin{matrix} =0 & \text{when } i \neq j \\ =1 & \text{when } i = j \end{matrix} \right)$$

Combining the orthogonality relation (equation (56)) with the integral equation (53), a different type of orthogonality relation can be derived as follows. Let θ_r, θ_s by the slopes of the rth and sth buckled mode corresponding to the buckling load $\bar{P}_r$ and $\bar{P}_s$ respectively. Then from equation (53),

$$\theta_r(x) = \bar{P}_r \int_0^1 r(x,\zeta)\theta_r(\zeta)d\zeta \tag{57}$$

$$\theta_s(x) = \bar{P}_s \int_0^1 r(x,\zeta)\theta_s(\zeta)d\zeta \tag{58}$$

Multiplying (57) by θ_s, (58) by θ_r, and integrating over the length of the beam,

$$\int_0^1 \theta_r\theta_s dx = \bar{P}_r \int_0^1 \int_0^1 r(x,\zeta)\theta_r(\zeta)\theta_s(x)dxd\zeta \tag{59}$$

$$\int_0^1 \theta_r\theta_s dx = \bar{P}_s \int_0^1 \int_0^1 r(x,\zeta)\theta_s(\zeta)\theta_r(x)dxd\zeta \tag{60}$$

In view of the symmetry of $r(x,\zeta)$, the above integrals are identical on both sides of the equation,

$$\int_0^1 \int_0^1 r(x,\zeta)\theta_r(\zeta)\theta_s(x)d\zeta dx = \frac{N_r}{\bar{P}_r}\delta_{rs} \tag{61}$$

Equation (61) yields a very interesting result when r is equated to s. That is

$$\bar{P}_r \approx \frac{N_r}{\int_0^1 \int_0^1 r(x,\zeta)\theta_r(\zeta)\theta_s(x)\,dxd\zeta} \qquad (62)$$

$$= \frac{\int_0^1 \theta_r^2(x)\,dx}{\int_0^1 \int_0^1 r(x,\zeta)\theta_r(\zeta)\theta_s(x)\,dxd\zeta}$$

This formula could be used to estimate the buckling load of the elastically restrained column.

Some Useful Results Derived from the Integral Equation Formulation

With regards to the kernel $r(x,\zeta)$ of the integral equation (53), the following observations are made:

(1) The kernel is symmetric with respect to x and ζ.

(2) The kernel is positive in the following sense.

$$I = \int_0^1 \int_0^1 r(x,\zeta)\theta(x)\theta(\zeta)\,dxd\zeta \geq 0 \qquad (63)$$

where θ is an arbitrary function. Equation (63) holds true because the integral quantity can be shown to be proportional to the strain energy which is obviously positive. At this stage it is convenient to

introduce orthonormal functions φ_i defined by

$$\varphi_i(x) = \frac{\theta_i(x)}{\sqrt{N_i}} \tag{64}$$

For $i = j$ equation (56) can be rewritten as

$$\int_0^1 \varphi_i^2(x) \, dx = 1$$

Because of the conditions given above for the kernel, it follows from Mercer's theorem [15] that the kernel can be expanded in terms of the orthonormal functions and the eigenvalues as follows:

$$r(x,\zeta) = \sum_{i=1}^{\infty} \frac{\varphi_i(\zeta)\varphi_i(x)}{\bar{P}_i} \tag{65}$$

Equation (65) yields many interesting relations which connect the buckling load and the behavior of the beam under the non-destructive force system. When it is combined with the orthogonality relation (equation (61)) it gives two kinds of infinite sum relationship for the eigenvalues.

The first is obtained by letting $x = \zeta$ in equation (65) and integrating over the span

$$\int_0^1 r(x,x)dx = \sum_{i=1}^{\infty} \int_0^1 \frac{\theta_i^2(x)}{\bar{P}_i N_i} dx = \sum_{i=1}^{\infty} \left(\frac{1}{\bar{P}_i}\right) \tag{66}$$

the second by integrating $r^2(x,\zeta)$ with respect to both x and ζ.

$$\int_0^1 \int_0^1 r^2(x,\zeta)dxd\zeta = \sum_{i=1}^{\infty} \left(\frac{1}{\bar{P}_i N_i}\right)^2 \int_0^1 \theta_i^2(x)dx \int_0^1 \theta_i^2(\zeta)d\zeta = \sum_{i=1}^{\infty} \left(\frac{1}{\bar{P}_i}\right)^2 \tag{67}$$

These two results will be discussed later. Other interesting relations can be derived from equation (65). By definition

$$r(x,\zeta) = \frac{\partial^2 C(x,\zeta)}{\partial x \partial \zeta} = \sum_{i=1}^{\infty} \frac{\theta_i(x)\theta_i(\zeta)}{\bar{P}_i N_i} \tag{68}$$

Integrating with respect to ζ gives

$$\frac{\partial \bar{C}(x,\zeta)}{\partial x} = \sum_{i=1}^{\infty} \frac{\theta_i(x)w_i(\zeta)}{\bar{P}_i N_i} + f(x) \tag{69}$$

Integrating again with respect to x gives

$$\overline{C}(x, \zeta) = \sum_{i=1}^{\infty} \frac{w_i(x)w_i(\zeta)}{\overline{P}_i N_i} + F(x) + G(\zeta) \qquad (70)$$

From the reciprocal theorem,

$$F(x) \equiv G(x)$$

Then equation (70) can be rewritten as

$$\overline{C}(x, \zeta) = \sum_{i=1}^{\infty} \frac{w_i(x)w_i(\zeta)}{\overline{P}_i N_i} + F(x) + F(\zeta) \qquad (71)$$

Suppose the boundary restraint is such that the lateral movement is not allowed at $x = 0$, then in equation (71),

$$w_i(0) = 0, \qquad \overline{C}(0, \zeta) = 0$$

Hence,

$$F(0) + F(\zeta) = 0 \qquad \text{for} \quad 0 \leq \zeta \leq 1 \qquad (72)$$

This means that the unknown function F is identically zero. This argument holds true also when the lateral stiffness at $x = 1$ is infinite. Hence, equations (69) and (70), with this restriction, become

$$\theta(x,\zeta) = \frac{\partial \bar{C}(x,\zeta)}{\partial x} = \sum_{i=1}^{\infty} \frac{\theta_i(x)w_i(\zeta)}{\bar{P}_i N_i} \tag{73}$$

$$\bar{C}(x,\zeta) = \sum_{i=1}^{\infty} \frac{w_i(x)w_i(\zeta)}{\bar{P}_i N_i} \tag{74}$$

When the end lateral stiffness is finite, the function F represents the deflection caused by the rigid body rotation. Multiplying equation (73) by $\theta_i(x)$ and integrating with respect to x from 0 to 1 results in the following simple relation

$$\int_0^1 \theta(x,\zeta)\theta_i(x)dx = \frac{w_i(\zeta)}{\bar{P}_i} \tag{75}$$

Integration of equation (75) with respect to ζ from 0 to 1 yields

$$\int_0^1 \left[\int_0^1 \theta(x,\zeta)d\zeta \right] \theta_i(x)dx = \frac{\int_0^1 w_i(\zeta)d\zeta}{\bar{P}_i} \tag{76}$$

But,

$$\theta(x) = \int_0^1 \theta(x,\zeta)d\zeta \tag{77}$$

(Note that $\theta(x)$ is the slope at x due to a uniformly distributed load.)
Substitution of equation (77) into equation (76) gives

$$\bar{P}_i = \frac{\int_0^1 w_i(x)dx}{\int_0^1 \theta(x)\theta_i(x)dx} \tag{78}$$

Since the lowest buckling load P_1 ($= P_{cr}$) is of the prime interest,
equation (78) can be rewritten as

$$\bar{P}_{cr} = \frac{\int_0^1 w_1(x)dx}{\int_0^1 \theta(x)\theta_1(x)dx} \tag{79}$$

Application and Discussion of the Results Obtained in Section 3

The main purpose of studying the buckling problem in the integral
equation formulation is to search for the mathematical background for
those empirical formulae derived in Chapter II. The procedure adopted
was as follows.

The instability problem was set up in such a manner that the
critical loads were related to factors which define a non-destabilizing
force system. Now since such force factors systems appear in an integral
quantity, there must be a reasonable probability that a certain para-

meter (e.g., deflection, slope, characteristic length, etc) may be associated with this integral. If this is so, we may be able to derive laws of similar form to the empirical ones.

Following this reasoning infinite sum relations (equations (66) and (67)) were developed. These equations establish that integral quantities associated with a couple distributed along the span can be expressed as the infinite sums of the inverses of eigenvalues or their squares. Since the empirical law defined earlier is related to the lowest buckling load P_{cr}, these equations cannot be the answer to our problems unless the ratios of the sums of these infinite series to P_{cr} remain nearly constant. To clarify this point beams with equal rotational restraint and a lateral tip spring are considered. The summation is carried out over the first eight eigenvalues. The results are shown in Table 12 and 13. It is clear that these ratios vary widely. This means that the two equations do not explain the validity of the empirical law. Since the empirical formula which uses the characteristic length works extremely well for the case when the lateral stiffness is infinite, it is worthwhile to investigate equation (79) with the assumption of infinite lateral stiffness. In this case when the denominator is integrated by parts, the boundary terms vanish and equation (79) becomes

$$\bar{P}_{cr} = \frac{\int_0^1 w_1 \, dx}{-\int_0^1 w_{,xx} w_1 \, dx} \qquad (80)$$

Table 12. Sum of the Higher Eigenvalues of Rotationally Restrained Beam

$\frac{KL}{EI}$	① $\frac{P_{cr}L}{\pi^2 EI}$	② $\frac{1}{8}\sum_{i=1}^{8}\frac{P_i L^2}{\pi^2 EI}$	③ ②/①	④ $\sqrt[8]{\frac{1}{8}\sum_{i=1}^{8}\left(\frac{P_i L^2}{\pi^2 EI}\right)^2}$	⑤ ④/①
0	1.000	.655	.655	.961	.961
.1	1.040	.673	.647	.998	.960
.2	1.079	.691	.640	1.033	.957
.5	1.193	.741	.621	1.133	.950
1	1.367	.813	.595	1.285	.940
2	1.668	.930	.558	1.540	.923
3	1.917	1.021	.533	1.745	.910
5	2.297	1.154	.502	2.051	.893
8	2.678	1.287	.481	2.353	.879
10	2.854	1.349	.473	2.493	.874
15	3.146	1.455	.462	2.726	.866
20	3.322	1.522	.458	2.868	.863
30	3.521	1.602	.455	3.032	.861
100	3.845	1.740	.453	3.304	.859
10^5	3.999	1.809	.452	3.437	.859

Table 13. Sum of Eigenvalues for the Cantilever Beam With a Lateral Tip Spring.

①	②	③	④	⑤
$\dfrac{KL^3}{EI}$	$\dfrac{P_{cr}L^2}{\pi^2 EI}$	$\dfrac{1}{8}\sum\limits_{i=1}^{8}\dfrac{P_iL^2}{\pi^2 EI}$	$\dfrac{②}{①}$	$\dfrac{1}{8}\sum\limits_{i=1}^{8}\left(\dfrac{P_iL^2}{\pi^2 EI}\right)^2$	$\dfrac{④}{①}$
0	.250	.208	.832	.248	.993
1	.332	.262	.789	.327	.987
2	.412	.310	.751	.405	.981
3	.492	.353	.717	.479	.973
5	.648	.427	.659	.619	.956
10	1.009	.564	.559	.915	.907
16	1.364	.673	.494	1.175	.861
20	1.538	.726	.472	1.301	.846
24	1.662	.769	.463	1.398	.841
30	1.779	.819	.460	1.507	.847
40	1.877	.879	.468	1.623	.865
50	1.924	.921	.479	1.694	.880
70	1.969	.976	.496	1.770	.899
100	1.996	1.023	.513	1.821	.912
150	2.015	1.064	.528	1.854	.920
300	2.031	1.110	.546	1.880	.925
10⁷	2.046	1.142	.558	1.897	.927

Interpretation of the denominator in equation (80) becomes clear when the bending moment diagram under the uniformly distributed load, the buckled mode and the product of the two are drawn for two extreme cases, i.e., simply supported and clamped. It is shown in Figure 16. These pictures illustrate the fact that to evaluate the integral of the denominator of equation (80), the necessary range of integral is approximately (exact when simply supported) between two moment-zero locations. This indicates that the distance between the inflection points is an important parameter for the integral

$$\int_0^{\ell} w_{,xx} w_1 \, dx.$$

Although this is not a proof of the validity of the empirical formula, it definitely explains why the distance between two inflection points is an important parameter in the uniform load cases considered. To broaden the basis of study there are two questions which arise. Is the demonstration restricted to a uniformly distributed load? Is it possible also to illustrate the mathematical foundation of "P-delta", "P-theta" and some other empirical formula corresponding to a different kind of loading? As was shown in Chapter II, the "P-theta" method can be reduced to the characteristic length relation equation (21). Since a concentrated lateral force is used in "P-theta" and "P-delta" and equation (75) is the relation connecting the buckling and the behavior of the beam under a concentrated lateral force, this equation will be examined closely. Letting $i = 1$ in equation (75),

Simply Supported   Clamped

w_1

.25L

M

.211 L

$w_1 M$
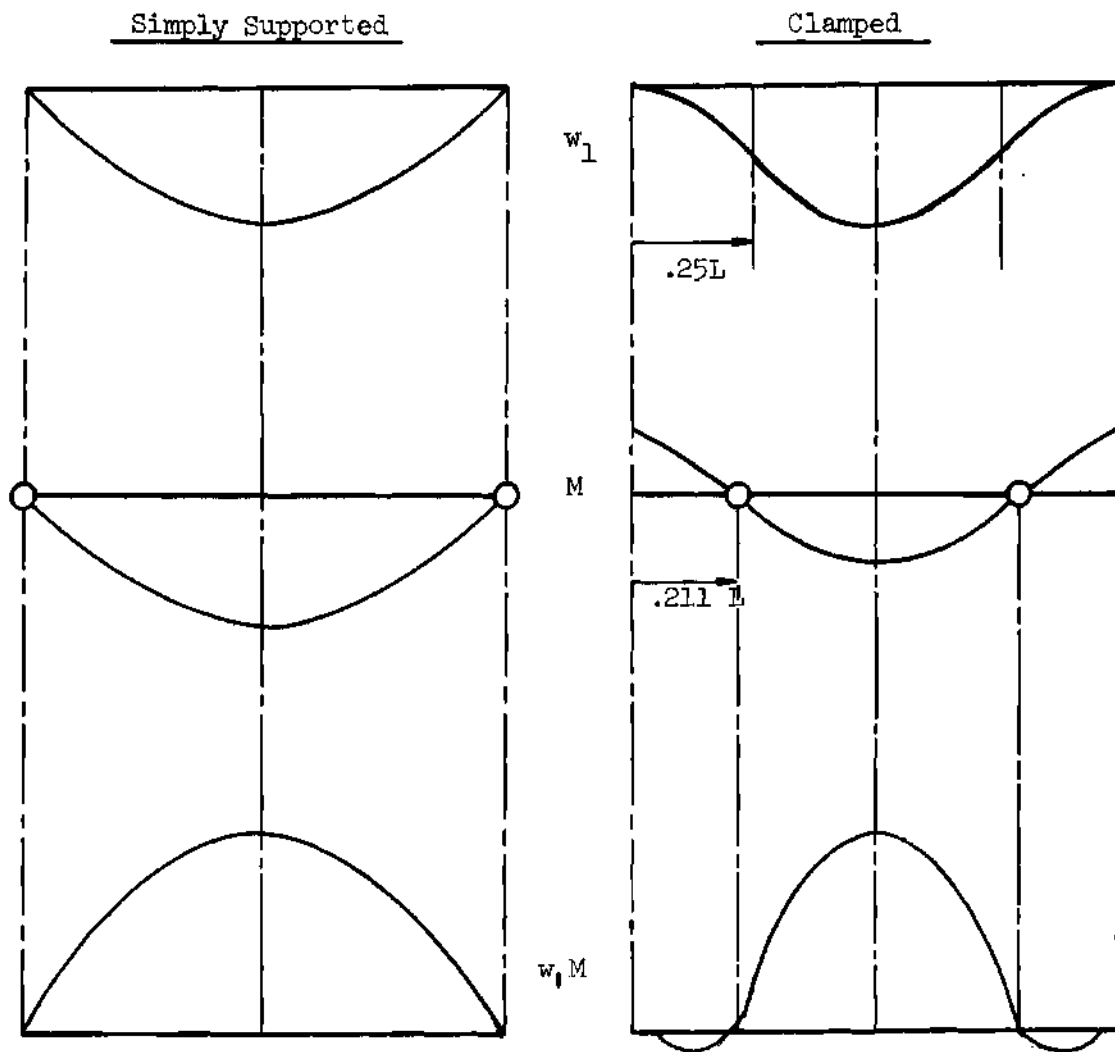
Figure 16. Illustration of the Product $w_1 M$ for Two Ideal Cases.

the following relation is obtained

$$\bar{P}_{cr} = \frac{w_1(\zeta)}{\int_0^1 \theta(x,\zeta)\theta_1(x)dx} \tag{81}$$

where

P_{cr} = the lowest buckling load

$\theta(x,\zeta)$ = slope at x due to a concentrated lateral force at ζ

$\theta_1(x)$, $w_1(x)$ = slope and deflection of the first buckled mode, respectively.

When the lateral restraint on the boundaries is infinite, equation (81) can be reduced to the following form:

$$\bar{P}_{cr} = \frac{w_1(\zeta)}{-\int_0^1 M(x,\zeta)w_1(x)dx} \tag{82}$$

where $M(x,\zeta)$ is the moment at x due to a concentrated lateral force applied at ζ.

To make the argument simple, consider the beam with equal rotational restraint. It was shown in reference [6] that to apply the "P-delta" or "P-theta" method to this configuration a concentrated lateral force must be applied at the mid-point of the beam. The bending moment diagram due to a concentrated lateral load at $x = \frac{1}{2}$,

the buckled mode and the product of the two are drawn in Figure 17

for two extreme cases, i.e., simply supported and clamped.

These figures indicate that the denominator of equation (82)

can be reasonably evaluated between the inflection points.
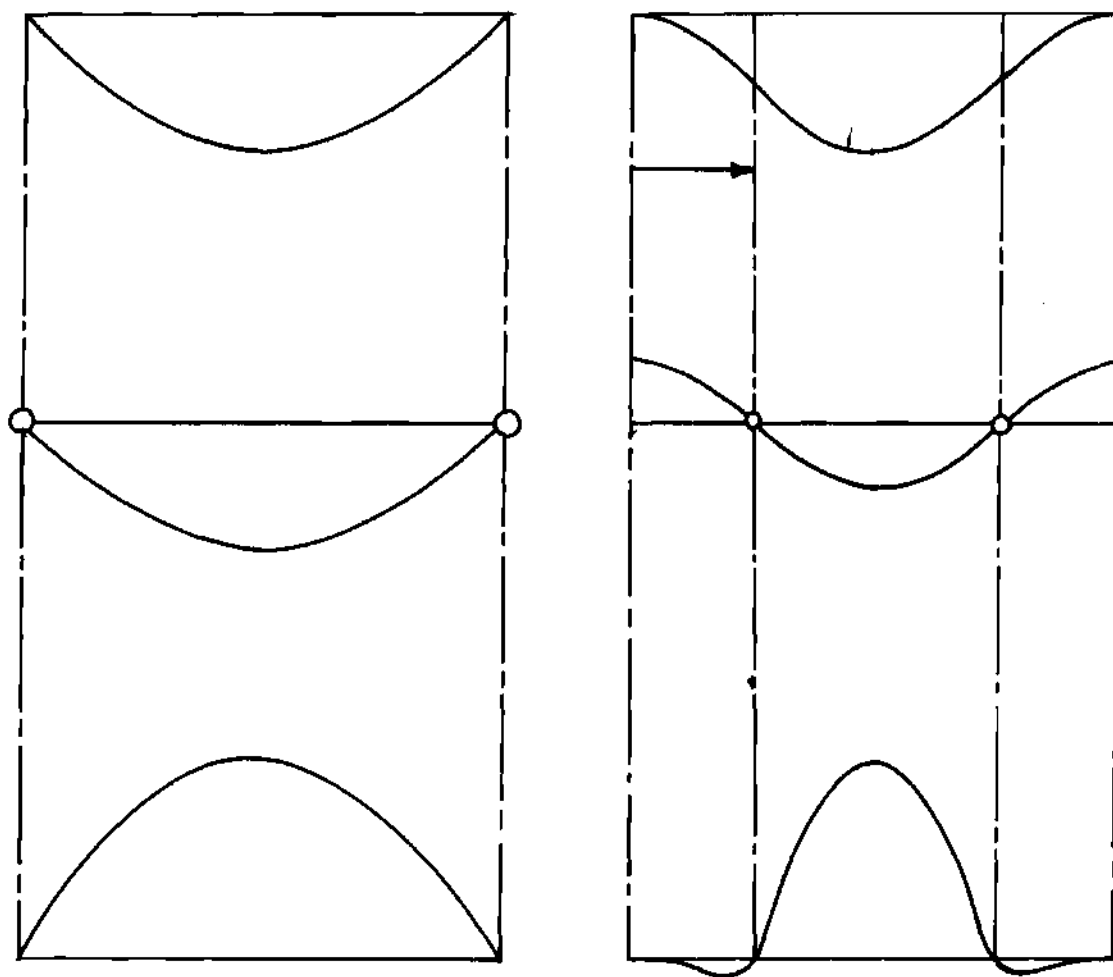
Figure 17 . Illustration of the Figure Mw.

CHAPTER IV

FURTHER CONSIDERATION OF THE BEAM COLUMN

The analysis of Chapter III has shown beyond doubt that the inflexion point separation distance for the laterally loaded column is an important parameter for describing the stability behavior. However, it has not generated a process which be used to analytically derive the results obtained by numerical analysis. It does serve, however, to emphasize that the key to the question may well lie in a study of the combined load problem.

In this chapter, therefore, we examine the combined load issue from a somewhat different viewpoint - in essence we shall follow a stiffness approach. This is, of course, common in studies of structural frameworks.

We begin with the simplest of problems, viz the pin jointed beam column with a central concentrated lateral load (Figure 18). Taking an origin at the center, the bending moment at the point whose coordinate is X is,

$$M = \frac{1}{2}Q \ [\frac{L}{2} - X] + PW = -EIW'' \tag{82}$$

Let

$$k^2 = \frac{P}{EI} \tag{83}$$
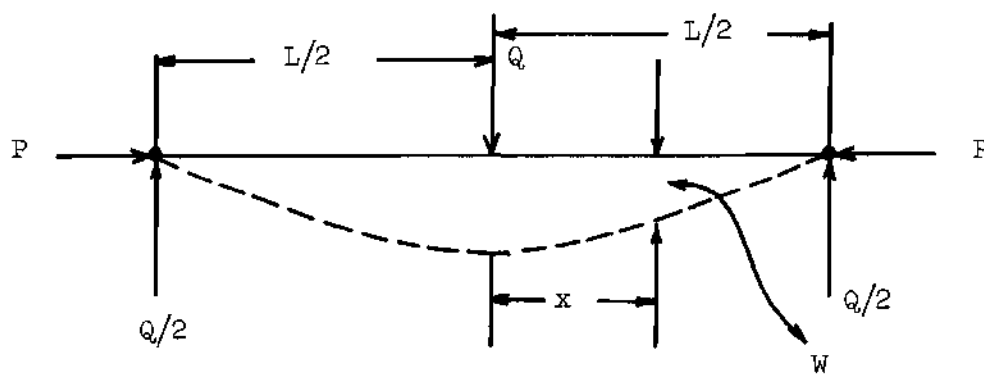
Figure 18. Pin Jointed Beam Column with a Central Concentrated Lateral Load.

therefore,

$$W'' + k^2 W = -\frac{Q}{EI} [\frac{L}{4} - \frac{X}{2}] \tag{84}$$

The solution is

$$W = A \sin kX + B \cos kX - (\frac{Q}{P})(\frac{L}{4} - \frac{X}{2}) \tag{85}$$

The boundary conditions are

$$\text{at} \quad X = 0 \qquad W' = 0 \tag{86a}$$

$$\text{at} \quad X = \frac{L}{2} \qquad W = 0 \tag{86b}$$

Using these boundary conditions in equation (85), we can write

$$W = \frac{QL}{2P} \left[-\frac{\sin kX}{kL} + \frac{\tan \frac{1}{2} kL \cos kX}{kL} - \left(\frac{1}{2} - \frac{X}{L}\right) \right] \tag{87}$$

The maximum deflection occurs at $X = 0$, and is given by

$$W_{max} = \frac{QL}{4P} \left[\frac{\tan \frac{1}{2} kL}{\frac{1}{2}kL} - 1 \right] \tag{88}$$

It can be seen that as P approaches $(\pi^2 EI)/(L^2)$, kL approaches π, and the application of a very small lateral load causes a very large deflection of the column. The stiffness of the column against lateral

displacement due to a transverse load at its center is

$$\frac{Q}{W_{max}} = \frac{4P}{L} \left\{ \frac{\frac{1}{2}kL}{\tan\frac{1}{2}kL - \frac{1}{2}kL} \right\} \tag{89}$$

The variation in stiffness with end load is very nearly linear.

When we treat the somewhat more complex case of the column with built in ends we find that for this case

$$W_{max} = \frac{Q}{2kP} \cdot \tan\frac{kL}{4} + \frac{Q}{P}\left(\frac{1}{2k}\right) \tan\frac{kL}{4} - \frac{L}{4} \tag{90}$$

or

$$W_{max} = \frac{Q}{kP} \left\{ \tan\frac{kL}{4} - \frac{kL}{4} \right\} \tag{91}$$

and so we have that

$$\frac{Q}{W_{max}} = \frac{(kL/4)}{\tan\frac{1}{4}kL - \frac{1}{4}kL} \cdot \frac{4P}{L} \tag{92}$$

It is clear that if we change the variable k to k_1 such that

$$k = 2k_1 \tag{93}$$

Then we may write

$$\frac{Q}{W_{max}} = \left(\frac{k_1 L/2}{\tan \frac{k_1 L}{2} - \frac{k_1 L}{2}}\right) \cdot \frac{4P}{L} \qquad (94)$$

and it is clear that the two stiffness lines are parallel curves, and the ratios of their intercepts with the axis are thus constant.

That equations (88) and (94) are to a close degree linear can be demonstrated in the following manner. Expand the tangent

$$\frac{\tan \frac{kL}{2}}{\frac{kL}{2}} = \frac{\tan \sqrt{\frac{PL^2}{4EI}}}{\sqrt{\frac{PL^2}{4EI}}} = 1 + \frac{1}{3}\left(\frac{PL^2}{4EI}\right) + \frac{2}{15}\left(\frac{PL^2}{4EI}\right)^2 + \frac{17}{315}\left(\frac{PL^2}{4EI}\right)^3 + \cdots \qquad (95)$$

Then, the expression for W_{max}, equation (88) may be written

$$W_{max} = \frac{QL}{4P}\left\{\frac{1}{3}\left(\frac{PL^2}{4EI}\right) + \frac{2}{15}\left(\frac{PL^2}{4EI}\right)^2 + \frac{17}{315}\left(\frac{PL^2}{4EI}\right)^3 + \cdots \right\} \qquad (96)$$

or

$$W_{max} = \frac{QL^3}{48EI}\left\{1 + \frac{3}{1}\cdot\frac{2}{15}\left(\frac{PL^2}{4EI}\right) + \frac{3}{1}\cdot\frac{17}{315}\left(\frac{PL^2}{4EI}\right)^2 + \cdots \right\} \qquad (97)$$

This is convergent if

$$\frac{2}{5}\frac{PL^2}{4EI} < 1; \text{ i.e. if } \frac{PL^2}{4EI} < \frac{5}{2} \simeq \frac{\pi^2}{4}$$

or if
$$P < P_{cr} \qquad (98)$$

In these circumstances the series may be replaced by a geometrical progression.

$$W_{max} = \frac{QL^3}{48EI} \left\{ 1 + \frac{PL^2}{10EI} + \left(\frac{PL^2}{10EI}\right)^2 + \ldots \right\}$$ (99)

This summed to infinity, gives

$$W_{max} = \frac{QL^3}{48EI} \cdot \frac{1}{1 - \frac{PL^2}{10EI}}$$

$$= \frac{QL^3}{48EI} \cdot \frac{1}{1 - \frac{P}{P_{cr}}}$$

or

$$W_{max} = \frac{QL^3}{48EI} \cdot \frac{P_{cr}}{P_{cr} - P}$$ (100)

The pin jointed strut with a uniformly distributed lateral load of intensity q and carrying an axial load of P is a classic problem. For this the bending moment at any point is given by

$$M = \frac{q}{k^2} \left(1 - \cos kx \sec \frac{kL}{2} \right)$$ (101)

with the convention given in Figure 18 . Thus

$$W' = \theta = \frac{q}{k^2} \int (1 - \cos kx \sec \frac{kL}{2}) dx + constant$$ (102)

Now the slope is maximum at the ends and zero in the center, so

$$\theta = \frac{q}{k^2} x + \frac{q}{k^3} \sin kx \sec \frac{kL}{2} \tag{103}$$

Thus

$$\theta_{max} = \frac{q}{k^2} \frac{L}{2} + \frac{q}{k^3} \tan \frac{kL}{2} \tag{104}$$

or

$$\theta_{max} = \frac{qL}{2k^2} \{1 + \frac{\tan \frac{kL}{2}}{\frac{kL}{2}}\} \tag{105}$$

This is very close to a linear relationship between compressive force and slope.

As the ends become restrained the expression for slope parameter becomes increasingly involved. For the encastré strut with uniform lateral load, the bending moment is given by

$$M = (M' - \frac{q}{k^2}) \sec \frac{kL}{2} \cos kx + \frac{q}{k^2} \tag{106}$$

where

$$M' = qk^2 \{1 - \frac{\frac{1}{2}kL}{\tan\frac{1}{2}kL}\} \tag{107}$$

Thus the slope expression is

$$\theta = \frac{1}{k}[M' - \frac{q}{k^2}] \sec \frac{kL}{2} \sin kx + \frac{q}{k^2} x \tag{108}$$

and the maximum value occurs when

$$\cos kX = - \frac{\dfrac{q}{k^2}}{\left(M' - \dfrac{q}{k^2}\right)\sec \dfrac{kL}{2}} \qquad (109)$$

The expression for θ/L becomes most complex and can only be evaluated numerically. When this is done we find that the relationship between θ/L and P is again linear and the slope of the line closely approximates that of the previous case.

We note further that when we examine the case of the column with an end moment the relationships developed differ from those previously desired. For the pin-ended column (Figure 18) we obtain

$$\frac{M_A}{\theta_A} = \left(\frac{EI}{L}\right) S(1 - c^2) \qquad (110)$$

where

$$S^* = \frac{(1 - kL \cot kL)\frac{1}{2}kL}{\tan\frac{1}{2}kL - \frac{1}{2}kL} \qquad (111)$$

and

$$C^* = \frac{kL - \sin kL}{\sin kL - kL \cos kL} \qquad (112)$$

---

* These quantities have been termed stability functions, see reference [17].

The variation of stiffness with end load is given in Figure 19.
For the fixed ended column (Figure 20(a)) the relationship is a little
simpler, viz

$$\frac{M}{\theta} = (\frac{EI}{L}) \cdot s \tag{113}$$

The graph of M/θ against $(P)/(\pi^2 EI/L^2)$ is shown in Figure 20(b). We note
immediately here that the curves are no longer parallel and thus we
should not anticipate being able to generate a viable relationship.
Pure numerical techniques as used in the first part of this thesis
failed to generate any results of value. It seems likely then that the
reason why the simple relationship can be found lies in the fact that
the variation of the pertinent stiffness parameters with respect to the
applied compressive force is essentially linear and the lines have
a slope which is independent of the degree of end fixity. The complexity
of the expressions is however such that at this time we have not been
able to verify this by other than numerical techniques. The reason
is clear. It is not easy to find simple, accurate algebraic approxi-
mations to the various transcendental functions involved. Whether or
not it will be possible in due course to demonstrate these conjectures
is open to question. Approximation analysis, like engineering, is
after all partly science, partly art.
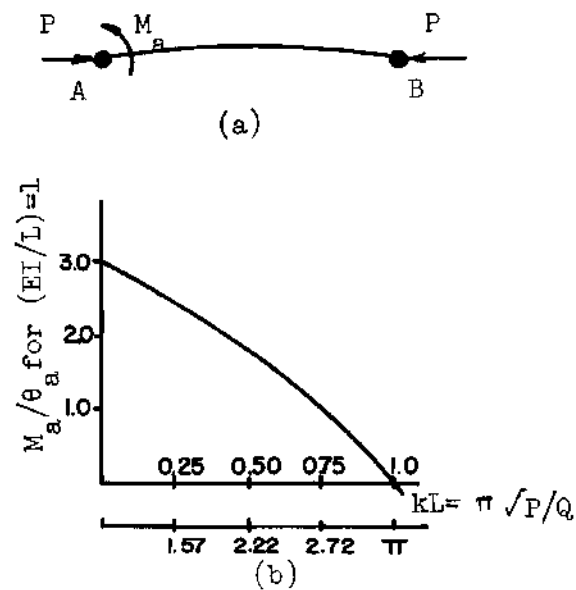
Figure 19. (a) Pin-ended Column. (b) Stiffness Plot
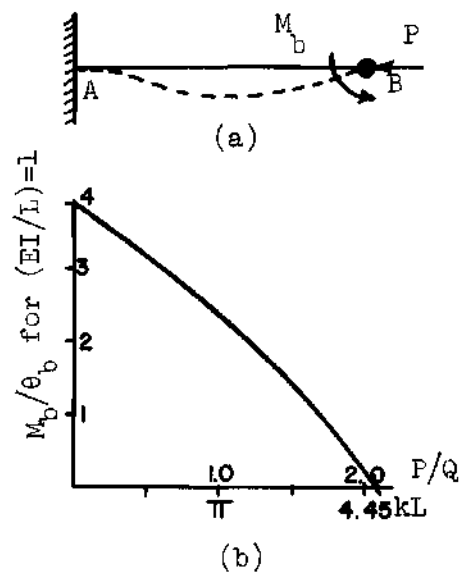
Figure 20. Fixed ended column

CHAPTER V

DESIGN FORMULAE FOR COLUMNS WITH ENDS PARTIALLY RESTRAINED

AGAINST ROTATION

Now that a practical method for determining the fixity which exists at the ends of columns has been devised it is important to the practising engineer that simple formulae for critical load in terms of end restraint be avilable.

The simplest of these laws, clearly, emanates from the Pδ law. It is shown in equation (32) Appendix A that for the column with equal end constraints that the deflection δ, due to a unit central lateral load is

$$\delta = \frac{\alpha + 8}{\alpha + 2} \cdot \frac{1}{192} \cdot \frac{L^3}{EI}$$

where $\alpha = K/EI$; K being the rotational stiffness of the end springs.

Thus, the critical load for such a column is given by

$$P_{cr} = \frac{4\pi^2 EI}{L^2} \cdot \left\{\frac{\alpha + 2}{\alpha + 8}\right\} \tag{114}$$

and, in the more general case of unequal end fixities α,β by

$$P_{cr} = \frac{4\pi^2 EI}{L^2} \cdot \sqrt{\frac{\alpha+2}{\alpha+8} \cdot \frac{\beta+2}{\beta+8}} \tag{115}$$

This latter result follows by virtue of the fact that the critical load for a column with unequal end rotational restraints α and β can be shown arithmetically, to a close approximation, to be the geometric mean of the critical loads of columns with end restraints α and β, respectively.

The derivation of an equally simple formula from the relationship between critical load level and the distance apart of the extremum points is not feasible. The complication arises from the fact that the expression for this quantity is a surd in the end restraint parameter.

It is of interest to note that when a Rayleigh quotient approach is taken to the solution of the same problem the following formulae can be derived:

$$P_{cr} = \frac{40EI}{L^2} \cdot \frac{\alpha^2 + 10\alpha + 16}{\alpha^2 + 14\alpha + 64} \tag{116}$$

and

$$P_{cr} = \frac{42EI}{L^2} \cdot \frac{\alpha^2 + 14\alpha + 24}{\alpha^3 + 18\alpha + 102} \tag{117}$$

The former (116) is derived by taking the column buckling deflection function to be identical with that due to a concentrated lateral load applied at the mid-point of the column, the latter on the assumption that the deflection curve corresponds to the displacement produced by a uniformly distributed side load.

Comparison of these Rayleigh formulae and the exact results

derived numerically from the characteristic equation is made in Table 14 .

It is clear from this table that the first expression is the closest approximation. It is interesting to note that the percentage of error is very nearly constant over a wide range of end stiffnesses. This suggests that we might divide the constant by a number close to unity and obtain an adjusted formula of greater accuracy. Indeed, when the formula is written as

$$P_{cr} = \frac{4\pi^2 EI}{L^2} \cdot \frac{\alpha^2 + 10\alpha + 16}{\alpha^2 + 14\alpha + 64} \tag{118}$$

the maximum error is reduced to .6 percent as can be deduced from Table 14, and of course the extreme values ($\alpha = 0$ and $\alpha = \infty$) are exact.

This is an interesting expression because it can be written

$$P_{cr} = \frac{4\pi^2 EI}{L^2} \cdot \frac{(\alpha+2)(\alpha+8)}{(\alpha+8)^2 - 2\alpha} \tag{119}$$

$$= \frac{4\pi^2 EI}{L^2} \cdot \frac{\alpha+2}{(\alpha+8) - \frac{2\alpha}{\alpha+8}}$$

$$= \frac{4\pi^2 EI}{L^2} \cdot \frac{\alpha+2}{\alpha+8} \left\{ 1 + \frac{2\alpha}{(\alpha+8)^2} \right\}$$

Now clearly $\frac{2\alpha}{(\alpha+8)^2}$ is small for all values of α between 0 and ∞.

Table 14. Approximation by Rayleigh's Quotient - Rotational Restraints

$\dfrac{KL}{EI}$	$\dfrac{P_{cr}L^2}{\pi^2 EI}$	Concentrated Lateral Force		Uniformly Distributed Load	
		$\dfrac{P_{est}L^2}{\pi^2 EI}$	Error (%)	$\dfrac{P_{est}L^2}{\pi^2 EI}$	Error (%)
0	1.000	1.013	1.3	1.013	.1
0.1	1.040	1.054	1.3	1.042	.1
1	1.367	1.385	1.3	1.372	.3
2	1.669	1.689	1.2	1.678	.5
3	1.921	1.938	.9	1.934	.7
5	2.298	2.320	.9	2.334	1.5
8	2.683	2.702	.7	2.745	2.3
10	2.854	2.880	.9	2.941	3.0
15	3.147	3.176	.9	3.272	4.0
20	3.327	3.356	.9	3.475	4.5
30	3.527	3.561	1.0	3.709	5.2
40	3.633	3.674	1.1	3.837	5.6
50	3.702	3.745	1.2	3.918	5.8
60	3.748	3.794	1.2	3.973	6.0
80	3.810	3.856	1.2	4.042	6.1
100	3.845	3.894	1.3	4.085	6.1
1000	3.984	4.037	1.3	4.238	6.4
10000	3.998	4.051	1.3	4.254	6.4

Thus, the expression of equation (118) is reduced to

$$P_{cr} = \frac{4\pi^2 EI}{L^2} \cdot \frac{\alpha+2}{\alpha+8} \qquad (114)\text{bis}$$

which is identical to that previously derived from the Pδ law.

The approximation formula given in equation (117) can be likewise adjusted. To do this we again ensure compliance at the extremes and hence write

$$P_{cr} = \frac{4\pi^2 EI}{L^2} \left\{ \frac{\alpha^2 + 14\alpha + 24}{\alpha^2 + 18\alpha + 96} \right\} \qquad (119)$$

which after suitable algebraic manipulation becomes

$$P_{cr} = \frac{4\pi^2 EI}{L^2} \left\{ \frac{\alpha+2}{\alpha+8} \right\} \left\{ 1 + \frac{2\alpha}{(\alpha+8)(\alpha+12)} \right\} \qquad (120)$$

which for all practical purposes is again

$$P_{cr} = \frac{4\pi^2 EI}{L^2} \left(\frac{\alpha+2}{\alpha+8} \right) \qquad (114) \text{ bis}$$

since $\frac{2\alpha}{(\alpha+8)(\alpha+12)}$ is very small for all values of α.

Thus we can see that the Pδ law and in all probability the others also would be analytically derivable if we could develop approximation method for deriving or expressing all relevant stability and other parameters in simple algebraic terms.

For the cantilever beam with a lateral tip spring neither the uniformly distributed load nor the concentrated lateral force deflection curves give a reasonable estimate of the buckling load when used in the Rayleigh formulation. This is not surprising because neither curve is a close representation of the deflection shape. The deflection produced by an end couple is much more similar to that which results from instability. When this deflection shape is used a quadratic rational function can be developed for the critical load viz

$$\bar{P}_{cr} = 30 \left\{ \frac{\beta^2 + 15\beta + 36}{\beta^2 + 15\beta + 360} \right\} \frac{EI}{L^2} \qquad (121)$$

It is clear that this expression is a poor representation because when $\beta = 0$ the value must be $(\pi^2 EI)/(4L^2)$ whereas the expression in equation (121) gives $(3EI)/(L^2)$. Similarly when $\beta = \infty$ the critical load is $(2.05\pi^2 EI)/(L^2)$ whereas the above formula yields $(30EI)/(L^2)$ or $(3\pi^2 EI)/(L^2)$. The maximum error in the estimation, in fact, amounts to 50 percent. However, when the approximate expression is plotted against the exact values on a log-log plot it is found that

$$P_{cr} = .740 \left(30 \frac{\beta^2 + 15\beta + 36}{\beta^2 + 15\beta + 360} \right)^{.912} \qquad (122)$$

is a very good approximation. The log-log plot is shown in Figure 21 and a comparison between the approximation of equation (122) and the exact values is given in Table 15.

Table 15. Approximation of the Buckling Load Using Rayleigh's Quotient-Modified-Lateral Tip Spring Case.

| $\dfrac{KL^3}{EI}$	$\dfrac{P_{crt}L^2}{EI}$	Approximation According to Eq.(122)	
		$\dfrac{P_{est}L^2}{EI}$	Error(%)
0	.250	.250	.0
0.5	.291	.293	.7
1	.332	.336	1.3
2	.412	.422	2.5
5	.648	.673	3.9
8	.870	.895	2.9
10	1.009	1.025	1.6
14	1.257	1.238	-1.5
18	1.457	1.401	-3.9
20	1.538	1.466	-4.6
24	1.662	1.573	-5.3
30	1.779	1.689	-5.1
40	1.877	1.808	-3.7
50	1.924	1.878	-2.4
100	1.996	1.995	-0.1
500	2.037	2.044	.3
1000	2.042	2.045	.2
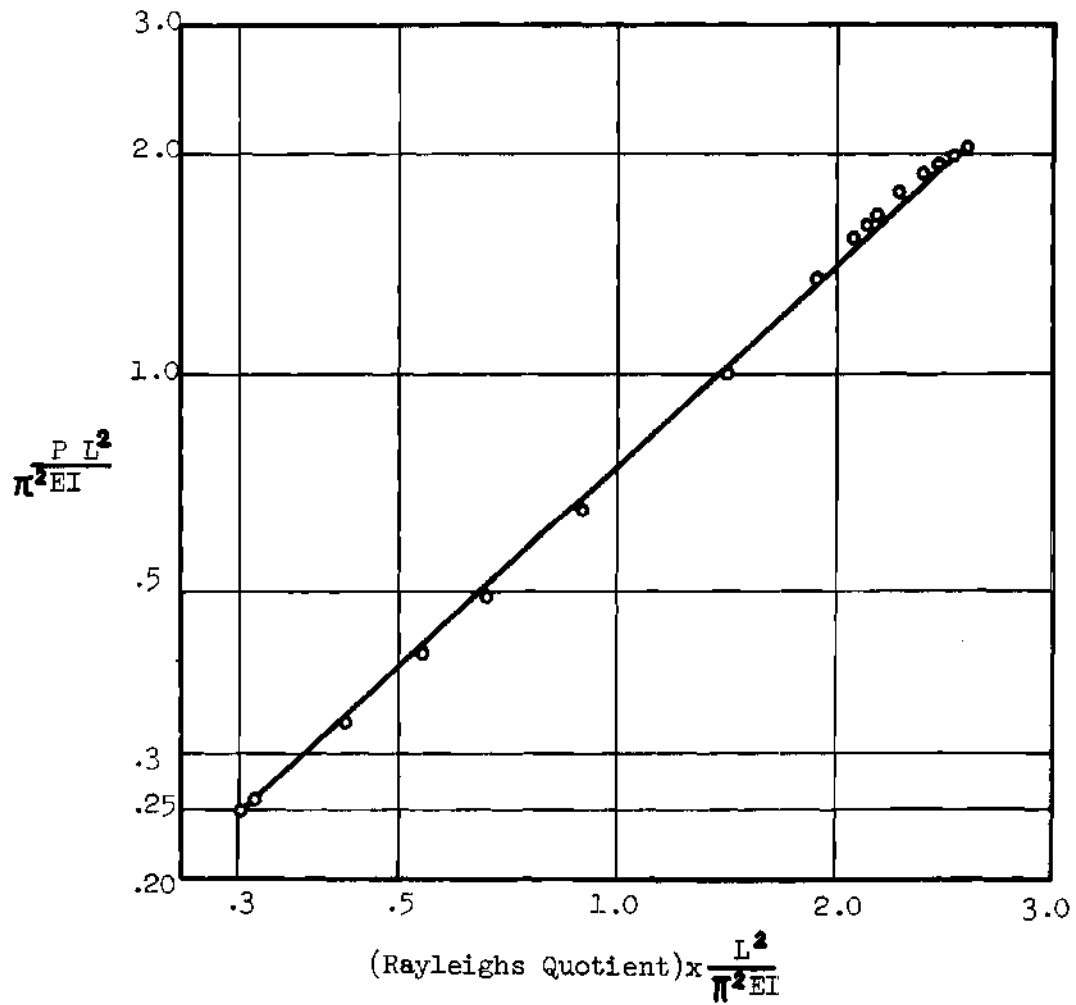
Figure 21. Correlation Curve between the Rayleigh's Quotient and the Buckling Load for the Lateral Tip Spring Case

CHAPTER VI

CONCLUSIONS

The analysis recorded in this thesis demonstrates clearly that simple relationships which couple the stability behavior of a column under axial compression and the distortions of an identical member under lateral force can be developed. These relationships appear to have importance in the non-destructive evaluation of existing column structures. It seems likely that they also provide a means whereby designers of column type structures, e.g. civil engineers might systematically develop end fixity systems of known performance which could be standardized. This would, of course, lead to an improvement in design.

Of particular interest in the format of the equation developed is that in many apparently four variable problems a single parameter, associated with the transverse loading situation, can be found to describe the critical load. This condition is not restricted to a single lateral load distribution but appertains in general. The parameter, however, distinctly varies with the distribution.

It is also pertinent to point out that for defined end fixity conditions the equations developed in the thesis are frequently capable of giving practicing engineers an approximation to critical load values as expeditiously as the Rayleigh-Ritz procedure and to an equal accuracy.

An effort to explain the success of the process led to further

study of the applicability of integral equation in the evaluation of eigenvalues for the column stability problem. This study showed that this technique is very applicable to the issue. General relationships that may be at least as powerful as the normal Rayleigh-Ritz expression were derived.

Although the empirical laws were not positively shown to have a solid foundation by analytic processes, the mathematical derivations clearly indicate that this would be demonstrated if appropriate approximation techniques could be developed.

APPENDIX A

ROTATIONALLY RESTRAINED BEAM ON LATERALLY UNYIELDING END SUPPORTS

Establishment of the Characteristic Equation for Instability

For the configuration shown in Figure 22a, the non-dimensionalized buckling equation is

$$w^{IV} + \lambda^2 w'' = 0 \tag{1}$$

The appropriate boundary conditions are

$$w = 0, \quad w'' - \alpha_o w' = 0 \qquad \text{at } x = 0 \tag{2}$$

$$w = 0, \quad w'' + \alpha_1 w' = 0 \qquad \text{at } x = 1$$

The general solution for equation (1) can be written as

$$w = A \sin \lambda x + B \cos \lambda x + Cx + D \tag{3}$$

The solution in conjunction with the boundary conditions yields the following buckling determinant:
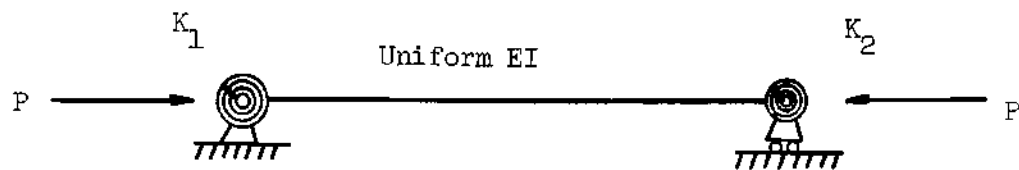
(a) Buckling
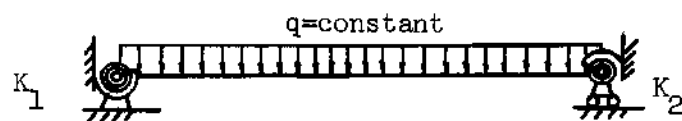
(b) Uniformly Distributed Load

Figure 22.   Rotationally Restrained Beam on
the Unyielding End Supports.

$$\begin{vmatrix} \alpha_o \lambda & \lambda^2 & \alpha_o \\ \sin \lambda & \cos\lambda - 1 & 1 \\ \alpha_1 \lambda\cos\lambda - \lambda^2\sin\lambda & -\alpha_1\lambda\sin\lambda - \lambda^2\cos\lambda & \alpha_1 \end{vmatrix} = 0 \qquad (4)$$

Expansion of this determinant gives the characteristic equation

$$\alpha_o\alpha_1[2(1-\cos\lambda) - \lambda\sin\lambda] - (\alpha_o + \alpha_1)\lambda(\lambda\cos\lambda - \sin\lambda) \qquad (5)$$

$$+ \lambda^3\sin\lambda = 0$$

Extremum Slope Relationship Under Uniformly

Distributed Lateral Load

The deflection and slope under a uniformly distributed lateral load are derived as follows. (see Figure 22) If a non-dimensional uniform load is defined as

$$\bar{q} = \frac{qL^3}{EI} \qquad (6)$$

then the non-dimensional differential equation for deflection w is

$$w^{IV} - \bar{q} = 0 \qquad (7)$$

and the appropriate boundary conditions are

$$w = 0 \quad \text{and} \quad w'' - \alpha_o w' = 0 \quad \text{at} \quad x = 0 \tag{8}$$

$$w = 0 \quad \text{and} \quad w'' + \alpha_1 w' = 0 \quad \text{at} \quad x = 1$$

Successive integrations of the differential equation (7) give

$$w''' = \bar{q}x + A \tag{9}$$

$$w'' = \frac{1}{2}\bar{q}x^2 + Ax + B$$

$$w' = \frac{1}{6}\bar{q}x^3 + \frac{A}{2}x^2 + Bx + C$$

$$w = \frac{1}{24}\bar{q}x^4 + \frac{A}{6}x^3 + \frac{B}{2}x^2 + Cx + D$$

where A, B, C, and D are constants. These four constants are obtained by satisfying the boundary conditions of equation (8). They are thus determined to be

$$A = -\frac{\bar{q}}{2}\left(1 + \frac{\alpha_o - \alpha_1}{\Delta}\right) \tag{10}$$

$$B = \frac{\bar{q}}{12\Delta}\alpha_o(\alpha_1 + 6)$$

$$C = \frac{\bar{q}}{12\Delta}(\alpha_1 + 6)$$

$$D = 0$$

where $\Delta = 12 + 4(\alpha_o + \alpha_1) + \alpha_o\alpha_1$.

Substitution of (10) into (9) yields the following result:

$$M(x) = \frac{\bar{q}}{12} \left[6x^2 - 6(1 + \frac{\alpha_o - \alpha_1}{\Delta})x + \frac{\alpha_o(\alpha_1 + 6)}{\Delta} \right] \quad (11)$$

$$\theta(x) = \frac{\bar{q}}{12} \left[2x^3 - 3(1 + \frac{\alpha_o - \alpha_1}{\Delta})x^2 + \frac{\alpha_o(\alpha_1 + 6)}{\Delta}x + \frac{\alpha_1 + 6}{\Delta} \right]$$

$$w(x) = \frac{\bar{q}}{24} \left[x^4 - 2(1 + \frac{\alpha_o - \alpha_1}{\Delta})x^3 + \frac{\alpha_o(\alpha_1 + 6)}{\Delta}x^2 + 2\frac{\alpha_1 + 6}{\Delta}x \right]$$

where $w(x)$, $\theta(x)$, $M(x)$ are the deflection, slope and moment, respectively.
The locations of the extremum slope are obtained by solving $M(x) = 0$.
The result is

$$x = \frac{1}{2}[Z \pm \bar{\ell}_{ext}] \quad (12)$$

where

$$Z = 1 + \frac{\alpha_o - \alpha_1}{\Delta}$$

and

$$\bar{\ell}_{ext} = \sqrt{(1 + \frac{\alpha_o - \alpha_1}{\Delta})^2 - \frac{2}{3}\frac{\alpha_o(\alpha_1 + 6)}{\Delta}} \quad (13)$$

$$= \text{the distance between two inflection points}$$

Define

$$x_1 = \tfrac{1}{2}(Z - \bar{\ell}_{ext}) \tag{14}$$

$$x_2 = \tfrac{1}{2}(Z + \bar{\ell}_{ext})$$

The meaning of x_1, x_2, $\bar{\ell}_{ext}$, and Z are easily understood from Figure 23 . In equation (12) in the main text, the significant parameter is the sum of the absolute values of the slopes at the zero moment points. We seek an alternate method of expressing this quantity. Hence, $24(\theta_{x=x_2} - \theta_{x=x_1})$ is to be evaluated. From (14), the following relationships hold:

$$x_1 + x_2 = Z \tag{15}$$

$$x_2 - x_1 = \bar{\ell}_{ext}$$

$$x_1 \cdot x_2 = \tfrac{1}{4}(Z^2 - \ell_{ext}^2) = \frac{\alpha_o}{6\Delta}(\alpha_1 + 6)$$

Thus

$$x_2^{\,2} - x_1^{\,2} = Z\bar{\ell}_{ext} \tag{16}$$

$$x_2^{\,3} - x_1^{\,3} = \bar{\ell}_{ext}^3 + \bar{\ell}_{ext}\,\frac{\alpha_o(\alpha_1 + 6)}{2\Delta}$$
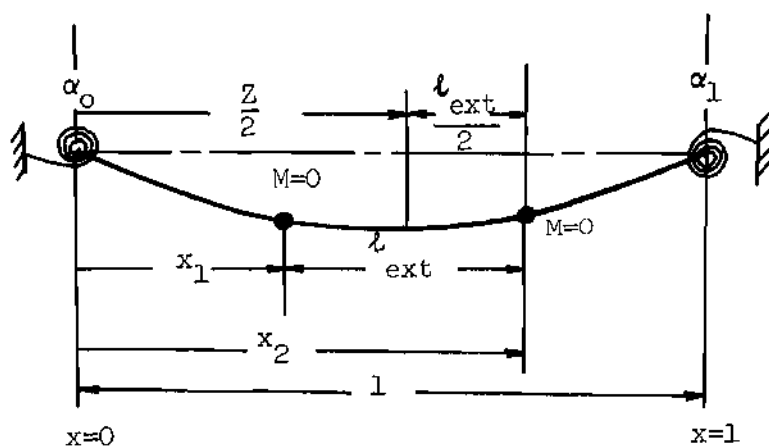
Figure 23. Illustration of x_1, x_2, ℓ_{ext} and Z.

Making use of this result,

$$\frac{24}{\bar{q}}(\theta_{x_2} - \theta_{x_1}) = \bar{\ell}_{ext}\left[4z^2 - \frac{4\alpha_o(\alpha_1 + 6)}{6\Delta} - 6z^2 + \frac{12\alpha_o(\alpha_1 + 6)}{6\Delta}\right] \qquad (17)$$

$$= \bar{\ell}_{ext}\left[-2z^2 + \frac{4\alpha_o(\alpha_1 + 6)}{3\Delta}\right] = -2\ell^3_{ext}$$

Establishment of Extremum Slope Relationship

Under Concentrated Lateral Force

The rotationally constrained beam as shown in Figure 3 is considered under a point lateral load Q applied at the location ζ. The non-dimensionalized governing differential equation and the boundary conditions are given by

$$w^{IV} - \bar{Q}\delta(x - \zeta) = 0 \qquad (18)$$

where

$$\bar{Q} = \frac{QL^2}{EI}$$

$$\text{at } x = 0 \qquad w = 0 \qquad (19)$$

$$w'' - \alpha_o w' = 0$$

$$\text{at } x = 1 \qquad w = 0 \qquad (20)$$

$$w'' + \alpha_1 w' = 0$$

The Laplace transform

$$w(s) = \int_0^\infty e^{-sx} w(x)dx \qquad (21)$$

is the most convenient tool to solve this problem.

Thus we derive

$$s^4 w(s) - [s^3 w(0) + s^2 w'(0) + s w''(0) + w'''(0)] - \bar{Q} e^{-\zeta s} = 0 \qquad (22)$$

Noting that $w(x) = 0$ at $x = 0$, (22) can be transformed back as follows:

$$w(x) = Ax + Bx^2 + Cx^3 = w_1(x) \text{ for } 0 \le x < \zeta \qquad (23)$$

$$w(x) = w_1(x) + \frac{\bar{Q}}{6}(x - \zeta)^3 \text{ for } \zeta \le x \le 1$$

where A, B, and C are constants. The constants A, B, and C are obtained from the boundary conditions (20). They are:

$$A = \bar{Q} \frac{\zeta(1 - \zeta)}{\Delta}[\alpha_1(1 - \zeta) + 2(2 - \zeta)] \qquad (24)$$

$$B = \bar{Q} \frac{\alpha_0 \zeta(1 - \zeta)}{2\Delta}[\alpha_1(1 - \zeta) + 2(2 - \zeta)]$$

$$C = -\bar{Q} \frac{1 - \zeta}{6\Delta} [3(\alpha_0 + 2)\{\alpha_1(1 - \zeta)+2\}-2(1 - \zeta)^2(\alpha_0+\alpha_1+\alpha_0\alpha_1)]$$

where $\Delta = 12 + 4(\alpha_0 + \alpha_1) + \alpha_0\alpha_1$.

Differentiation of equation (23) yields the slope and moment.

$$w' = A + 2Bx + 3Cx^2 = w_1'(x) \qquad \text{for } 0 \leq x < \zeta \qquad (25)$$

$$= w_1'(x) + \frac{\bar{Q}}{2}(x - \zeta)^2 \qquad \text{for } \zeta \leq x \leq 1$$

$$w'' = 2B + 6Cx = w_1''(x) \qquad \text{for } 0 \leq x < \zeta \qquad (26)$$

$$= w_1''(x) + \bar{Q}(x - \zeta) \qquad \text{for } \zeta \leq x \leq 1$$

Define

$$A = \tilde{A}\bar{Q}, \quad B = \tilde{B}\bar{Q}, \quad C = \tilde{C}\bar{Q} \qquad (27)$$

In the case where $\alpha_0 = \alpha_1 = \alpha$, ζ is $\frac{1}{2}$. Then $\tilde{B}$, $\tilde{C}$ are given by

$$\tilde{B} = \frac{\alpha}{16(\alpha + 2)} \qquad (28)$$

and

$$\tilde{C} = -\frac{1}{12}$$

The locations of extremum slope x_1 and x_2, are given by:

$$x_2 = \frac{\alpha}{4(\alpha+2)} \qquad (29)$$

$$x_1 = -\frac{\alpha}{4(\alpha+2)} + 1$$

Thus it follows that

$$x_2 - x_1 = \frac{\alpha + 4}{2(\alpha+2)} = \bar{\ell}_{ext} \qquad (30)$$

and

$$x_2 + x_1 = 1$$

The sum of the absolute values of the extremum slopes is

$$w'_{x=x2} - w'_{x=x1} = 2\tilde{B}(x_2-x_1) + 3\tilde{C}(x_2^2 - x_1^2) \qquad (31)$$

$$= \bar{\ell}_{ext}[2\tilde{B} + 3\tilde{C}(x_2 + x_1)]$$

$$= - \frac{\bar{\ell}^2_{ext}}{4}$$

The result is pertinent to the empirical law for the single concentrated load [7]. Substituting 1/2 for x in equation (23), deflection in the middle of the span is given as,

$$\delta = \frac{\alpha+8}{\alpha+2} \; \frac{1}{192} \; \frac{L^3}{EI} \qquad (32)$$

APPENDIX B

THE ELASTICALLY SUPPORTED BEAM COLUMN OF UNIFORM BENDING STIFFNESS

Differential Equation and Boundary Conditions

Consider an elastically supported beam column of uniform bending stiffness loaded with a distributed lateral force $q(X)$ and an axial compression force P as depicted in Figure 15. Let spring stiffnesses at the boundaries be K_1, K_2 for rotational restraint and K_3, K_4 for lateral restraint. Thus we may write the strain energy of the system as

$$U_i = \frac{1}{2} \int_o^L EI(w'')^2 \, dX + \frac{1}{2} \{ K_2 (w')^2 \big|_{X=L} + K_1 (w')^2 \big|_{X=0} + \tag{1}$$

$$+ K_3 w^2 \big|_{X=L} + K_4 w^2 \big|_{X=0} \}$$

and the work done by the external forces as

$$W_e = \frac{P}{2} \int_o^L (w')^2 dX + \int_o^L q(X) W dX \tag{2}$$

When the non-dimensional quantities defined below:

$$\alpha_o = \frac{K_1 L}{EI} \qquad \alpha_1 = \frac{K_2 L}{EI} \qquad (3)$$

$$\beta_o = \frac{K_4 L^3}{EI} \qquad \beta_1 = \frac{K_3 L^3}{EI}$$

$$w = \frac{W}{L}, \quad x = \frac{X}{L}, \quad \lambda^2 = \frac{PL^2}{EI}, \quad \bar{q} = \frac{qL^3}{EI}$$

are used; then non-dimensionalized strain energy and work functions can be written as

$$\bar{U}_i = \frac{1}{2} \int_0^1 (w'')^2 dx + \frac{1}{2}\alpha_o w'^2 \Big|_{x=0} + \frac{1}{2} \alpha_1 w'^2 \Big|_{x=1} \qquad (4)$$

$$+ \frac{1}{2} \beta_o w^2 \Big|_{x=0} + \frac{1}{2} \beta_1 w^2 \Big|_{x=1}$$

$$\bar{W}_e = \frac{\lambda^2}{2} \int_0^1 (w')^2 dx + \int_0^1 \bar{q}(x) \, w \, dx \qquad (5)$$

Total potential energy is:

$$U_T = \bar{U}_i - \bar{W}_e \qquad (6)$$

Thus the variation of total potential is

$$\delta U_T = \int_0^1 \{w^{IV} + \lambda^2 w'' - \bar{q}(x)\} \, \delta w \, dx + (w'' + \alpha_1 w') \, \delta w' \Big|_{x=1} \quad (7)$$

$$+ \, (-w'' + \alpha_o w') \, \delta w' \Big|_{x=0} + (-w''' - \lambda^2 w' + \beta_1 w) \delta w \Big|_{x=1}$$

$$+ \, (w''' + \lambda^2 w' + \beta_o w) \, \delta w \Big|_{x=0}$$

By equating δU_T to zero, the resulting differential equation and the boundary conditions are developed:

$$w^{IV} + \lambda^2 w'' - \bar{q}(x) = 0 \qquad (8)$$

$$\text{at } x = 0; \quad w'' - \alpha_o w' = 0 \text{ or } w' = 0 \qquad (9)$$

$$w''' + \lambda^2 w' + \beta_o w = 0 \text{ or } w = 0$$

$$\text{at } x = 1; \quad w'' + \alpha_1 w' = 0 \text{ or } w' = 0$$

$$w''' + \lambda^2 w' - \beta_1 w = 0 \text{ or } w = 0$$

Orthogonality Relation of the Buckled Mode

Let u, v be the buckled mode corresponding to the different eigenvalues λ and μ respectively. Then from (8)

$$u^{IV} + \lambda^2 u'' = 0 \qquad (10a)$$

$$v^{IV} + \mu^2 v'' = 0 \qquad (10b)$$

multiplying (10a) by v, (10b) by u and integrating the difference of the products from 0 to 1, the following integral is obtained.

$$I = \int_0^1 \left[(u^{IV} + \lambda^2 u'')v - (v^{IV} + \mu^2 v'')u \right] dx \qquad (11)$$

$$= \int_0^1 (u^{IV}v - uv^{IV})dx + \lambda^2 \int_0^1 u''vdx - \mu^2 \int_0^1 v''udx = 0$$

Integrating by parts and making use of the boundary conditions of equation (9), equation (11) can be reduced to the following simple relationship:

$$I = (\lambda^2 - \mu^2)\int_0^1 u'v'dx = 0 \qquad (12)$$

Therefore,

$$\int_0^1 u'v'dx = 0 \qquad (13)$$

Since

$$\lambda \neq \mu$$

This equation is an orthogonality relation of the buckled mode.

APPENDIX C

APPROXIMATION OF THE UNIFORMLY DISTRIBUTED LOAD SYSTEM

BY A FINITE NUMBER OF EQUALLY SPACED CONCENTRATED LATERAL FORCES

According to the result in Appendix A, the distribution of

moment along the constant cross-section beam on the unyielding end

supports subjected to a uniformly distributed lateral force is given by

$$m(x) = \frac{\bar{q}}{12}[6x^2 - 6(1 + \frac{\alpha_o - \alpha_1}{\Delta}) x + \frac{\alpha_o(\alpha_1 + 6)}{\Delta}] \qquad (1)$$

The distance between the inflection points $\bar{\ell}_{ext}$ is given by

$$\bar{\ell}_{ext} = \sqrt{(1 + \frac{\alpha_o - \alpha_1}{\Delta})^2 - \frac{2}{3} \frac{\alpha_o(\alpha_1 + 6)}{\Delta}} \qquad (2)$$

Suppose a beam of uniform EI is loaded with concentrated lateral

forces at the equally spaced intervals. The distance between the

inflection points under this loading system is to be found. According

to Appendix A, the moment distribution due to a lateral concentrated

force applied at loaction ζ is given by

$$m(x) = 2B + 6Cx \qquad \text{for } 0 \leq x < \zeta \qquad (3a)$$

$$= 2B + 6Cx + \bar{Q}(x-\zeta) \quad \text{for } \zeta \leq x \leq 1 \qquad (3b)$$

where

$$B = \frac{\bar{Q}}{2\Delta}[\alpha_o\alpha_1(\zeta - 2\zeta^2 + \zeta^3) + 2\alpha_o(2\zeta - 3\zeta^2 + \zeta^3)] \tag{4}$$

$$C = -\frac{\bar{Q}}{6\Delta}[\Delta - 6(\alpha_1 + 2)\zeta - 3\alpha_o(2 + \alpha_1)\zeta^2 + 2(\alpha_o + \alpha_1 + \alpha_o\alpha_1)\zeta^3]$$

Suppose the number of concentrated lateral forces is N. Then the location of the forces are

$$\zeta_i = \frac{i}{N + 1} \qquad\qquad i = 1, 2, \ldots, N \tag{5}$$

From equation (3b), the moment between the ith and the $(i+1)^{th}$ location is given by

$$m_{i \sim i+1} = \sum_{i=1}^{N} (2B_i + 6C_i x) + \bar{Q} \sum_{r=1}^{i} (x - \zeta_r) \tag{6}$$

where B_i and C_i are obtained by replacing ζ by ζ_i in B and C of equation (4). The following identities are used to calculate the summation in equation (6).

$$\sum_{i=1}^{n} i = \tfrac{1}{2}n(n + 1) \tag{7}$$

$$\sum_{i=1}^{n} i^2 = \frac{1}{6}n(n + 1)(2n + 1) \tag{8}$$

$$\sum_{i=1}^{n} i^3 = \frac{1}{4}n^2(n + 1)^2 \tag{9}$$

Thus

$$\sum_{i=1}^{N} \zeta_i = \frac{N}{2}, \quad \sum_{i=1}^{N} \zeta_i^2 = \frac{N(2N + 1)}{6(N + 1)}, \quad \sum_{i=1}^{N} \zeta_i^3 = \frac{N^2}{4(N + 1)} \tag{10}$$

The use of equation (10) in equation (6) yields the moment between i^{th} and $(i + 1)^{th}$ location.

$$m_{i \sim i+1} = \gamma + \rho x \tag{11}$$

where

$$\gamma = [\frac{\alpha_0(\alpha_1 + 6)}{12\Delta} \frac{N(N + 2)}{N + 1} - \frac{i(i + 1)}{2(N + 1)}]\bar{Q} \tag{12}$$

$$\rho = - \frac{\bar{Q}N}{2\Delta(N + 1)}[N(\alpha_0\alpha_1 + 5\alpha_0 + 3\alpha_1 + 12) + (\alpha_1 + 6)(\alpha_0 + 2)] + \bar{Q}i$$

If an inflection point exists in this region, it is located at

$$x = - \frac{\chi}{\rho}$$

Following this scheme, the distance between two inflection points was calculated. Then this length was used in the empirical formula (13) obtained in Chapter II to compare with the exact values of the critical loads. The computer program is shown in Appendix F and the results are listed in Table 11.

APPENDIX D

BEAM OF VARIABLE BENDING STIFFNESS

Clamped-Pinned Beam

Slope Evaluation

The slope at the pinned end of a beam loaded with a uniformly distributed load (q per unit length) is calculated. The differential equation for the lateral displacement W is given by

$$\frac{\partial^2}{\partial X^2}(EI(X)\, W") - q = 0 \tag{1}$$

Integrating (1) twice gives

$$EI(X)W" = \frac{q}{2}X^2 + \bar{A}X + \bar{B} \tag{2}$$

where $\bar{A}$ and $\bar{B}$ are constants. It is assumed that the bending stiffness is written in the form

$$EI(X) = EI_o\{1 - \frac{1}{T}(\frac{X}{L})^p\} \tag{3}$$

where T is a number greater than 1 and is called the taper ratio and p is a positive number. When the following non-dimensional quantities and conditions are introduced

$$x = \frac{X}{L} \qquad \bar{q} = \frac{qL^3}{EI_o} = 1 \qquad w = \frac{W}{L} \tag{4}$$

Equation (2) and the boundary conditions can be written as follows:

$$(1 - \frac{1}{T}x^P)w'' = \frac{1}{2}x^2 + Ax + B \tag{5}$$

where A and B are constants, and

$$w = 0 \qquad\qquad \text{at } x = 0 \tag{6a}$$

$$w' = 0 \qquad\qquad \text{at } x = 0 \tag{6b}$$

$$w = 0 \qquad\qquad \text{at } x = 1 \tag{6c}$$

$$w'' = 0 \qquad\qquad \text{at } x = 1 \tag{6d}$$

When the boundary condition (6d) is used in Equation (5), B can be expressed in terms of A. Thus,

$$B = -(A + \frac{1}{2}) \tag{7}$$

Hence (5) now is written as

$$(1 - \frac{1}{T}x^P)w'' = \frac{x^2}{2} + Ax - (A + \frac{1}{2}) \tag{8}$$

For the ease of calculation, only two cases (p = 1 and 2) are treated in detail.

Linearly Varying Bending Stiffness: p = 1. Equation (8) is now written as follows:

$$\frac{w''}{T} = \frac{1}{2}(\sigma - x) + \frac{\tau}{T - x} \tag{9}$$

where

$$\sigma = - (T + 2A) \tag{10}$$

$$\tau = \frac{T - 1}{2} (T + 2A + 1) \tag{11}$$

Integrating (9) yields

$$\frac{w'}{T} = - \frac{1}{4}(\sigma - x)^2 - \tau \ln (T - x) + C \tag{11}$$

When boundary condition (6b) is applied to equation (11), the constant C is obtained.

$$C = \frac{\sigma^2}{4} + \tau \ln(T) \tag{12}$$

Integrating (11) gives

$$\frac{w}{T} = \frac{1}{12} (\sigma - x)^3 + \tau(T - x)\left[\ln(T-x)-1\right]+Cx + D \tag{13}$$

and boundary condition (6a) is used to evaluate D.

$$D = - \frac{\sigma^3}{12} - \tau T \left[\ln(T)-1 \right] \qquad (14)$$

When (6c) is used in equation (13), the result is

$$\frac{1}{12}(\sigma - 1)^3 + \tau (T - 1)\left[\ln(T-1)-1\right]+\frac{\sigma^2}{4} + \tau \ln(T) - \frac{\sigma^3}{12} - \tau T\left[\ln(T)-1\right]=0 \qquad (15)$$

or

$$\tau(T - 1)\left[\ln(T - 1) -1\right] + \frac{\sigma}{4} - \frac{1}{12} + \tau \ln(T) - \tau T\left[\ln(T)-1\right]=0 \qquad (16)$$

From equation (10), τ can be related to σ as follows:

$$\tau = \frac{T - 1}{2} (1 - \sigma) \qquad (17)$$

Using (17) in (16) yields

$$(1 - \sigma)\left(\frac{(T-1)^2}{2} \ln\left(\frac{T-1}{T}\right) + \frac{2T - 3}{4}\right) + \frac{1}{6} = 0 \qquad (18)$$

From (11), the slope w' at $x = 1$ is

$$w' = T\left[-\frac{1}{2}(1 - \sigma) + \frac{1}{4} + \frac{T - 1}{2}(1 - \sigma)\ln\left(\frac{T}{T-1}\right)\right] \qquad (19)$$

When the values of $(1 - \sigma)$ which is calculated from (18) is used in

(19), the slope at the pinned end is obtained.

<u>Parabolically Varying Bending Stiffness: p = 2</u>. Let $\Lambda^2 = T$.

Then (8) is now

$$\frac{w''}{T} = -\frac{1}{2} + \frac{b}{\Lambda - x} + \frac{a}{\Lambda + x} \tag{20}$$

where

$$b = \frac{\Lambda - 1}{2\Lambda} \left[A + \frac{\Lambda + 1}{2}\right] \tag{21}$$

$$a = \frac{\Lambda + 1}{2\Lambda} \left[-A + \frac{\Lambda - 1}{2}\right] \tag{22}$$

When equation (20) is integrated and the boundary condition (6b) is used, the resulting equation is

$$\frac{w'}{T} = -\frac{x}{2} - b\ln(\Lambda - x) + a\ln(\Lambda + x) + A\ln\Lambda \tag{23}$$

Integration of equation (23) yields

$$\frac{w}{T} = -\frac{x^2}{4} + b(\Lambda - x)\left\{\ln(\Lambda - x) -1\right\} \tag{24}$$

$$+ a(\Lambda + x)\left\{\ln(\Lambda + x) - 1\right\} + xA\ln(\Lambda) + D$$

where the constant D is evaluated from the boundary condition (6a) as follows:

$$D = -(b + a)_\Lambda[\ln(\Lambda)-1] \qquad (25)$$

When the remaining boundary condition (6c) is used in equation (24), the result is

$$-\frac{1}{4} + A[1+ \ln\Lambda] + b[\Lambda\ln(\frac{\Lambda-1}{\Lambda})- \ln(\Lambda-1)] \qquad (26)$$
$$+ a[\Lambda\ln(\frac{\Lambda+1}{\Lambda})+ \ln(\Lambda+1)] = 0$$

Using (21) and (22) in (26), it is possible to write this equation in terms of the unknown constant A only. From which it follows that,

$$A = \frac{\frac{1}{4} - (\frac{\Lambda^2-1}{4\Lambda})[\Lambda\ln\ (\frac{\Lambda^2-1}{\Lambda^2}) + \ln\ (\frac{\Lambda+1}{\Lambda-1})]}{[1+ \frac{\Lambda^2+1}{2\Lambda}\ \ln\ (\frac{\Lambda-1}{\Lambda+1}) - \ln\ (\frac{\Lambda^2-1}{\Lambda^2})]} \qquad (27)$$

The slope at the pinned end is

$$w' = T\left[- \frac{1}{2} + b\ln(\frac{\Lambda}{\Lambda - 1}) + a\ln(\frac{\Lambda + 1}{\Lambda})\right] \qquad (28)$$

where b and a are as shown in (21) and (22).

Formulation of the Finite Difference Equation for Buckling Investigation

The buckling equation and the boundary conditions are

$$\frac{\partial^2}{\partial X^2}\left[EI(X)\frac{\partial^2 W}{\partial X^2}\right] + P\frac{\partial^2 W}{\partial X^2} = 0 \tag{29}$$

$$W = W' = 0 \quad \text{at } X = 0 \tag{30}$$
$$W = W'' = 0 \quad \text{at } X = L$$

As before, define

$$x = \frac{X}{L}, \quad w = \frac{W}{L}, \quad \lambda^2 = \frac{PL^2}{EI_o} \tag{31}$$

Then (29) and (30) become

$$\left\{(1 - \frac{1}{T}x^P)w''\right\}'' + \lambda^2 w'' = 0 \tag{32}$$

and

$$w = w' = 0 \quad \text{at } x = 0 \tag{33}$$
$$w = w'' = 0 \quad \text{at } x = 1$$

respectively. Completing the operation in (32) and introducing a new variable ($\eta = w''$), the following set of equations is obtained.

$$\left(1 - \frac{x^P}{T}\right)\eta'' + 2\left(-\frac{P}{T}x^{P-1}\right)\eta' + \left\{\lambda^2 - \frac{p(p-1)}{T}x^{P-2}\right\}\eta = 0 \tag{34}$$
$$\eta - w'' = 0$$

When the central difference is used to represent the derivatives, equation (34) can be reduced to the following finite difference equation.

$$\left(1 - \frac{1}{T}x_i{}^p\right)\left(\eta^{i+1} - 2\eta^i + \eta^{i-1}\right) - \frac{ph}{T}x_i{}^{p-1}\left(\eta^{i+1} - \eta^{i-1}\right) \qquad (35a)$$

$$+ h^2\left(\lambda^2 - \frac{p(p-1)}{T}x_i{}^{p-2}\right)\eta^i = 0$$

and, $$-h^2\eta^i + (w^{i+1} - 2w^i + w^{i-1}) = 0 \qquad (35b)$$

or in matrix form,

$$\lfloor A \rfloor \underline{z}^{i-1} + \lfloor B \rfloor \underline{z}^i + \lfloor C \rfloor \underline{z}^{i+1} = 0 \qquad (36)$$

where

$$\underline{z}^i = \left\{ \begin{array}{c} \eta^i \\ w^i \end{array} \right\} \qquad (37)$$

and

$$[A] = \begin{bmatrix} 1 - \frac{1}{T}\left(x_i^{\,p} - phx_i^{\,p-1}\right), & 0 \\ 0 & , & 1 \end{bmatrix} \qquad (38)$$

$$[B] = \begin{bmatrix} -2\left(1-\frac{1}{T}x_i^{\,p}\right) + h^2\left(\lambda^2 - \frac{p(p-1)}{T}x_i^{\,p-2}\right), & 0 \\ -h^2 & , & -2 \end{bmatrix}$$

$$[C] = \begin{bmatrix} 1 - \frac{1}{T}\left(x_i^{\,p} + phx_i^{\,p-1}\right), & 0 \\ 0 & , & 1 \end{bmatrix}$$

and h = size of division = 1/(number of division)

i denotes the i-th location,

for $1 \le i \le N-1$. Boundary matrices are formulated as follows:

at x = 0;

$$w_o' = \frac{1}{2h}(w_1 - w_{-1}) = 0, \therefore w_1 = w_{-1} \qquad (39)$$

then

$$\eta_0 = \frac{1}{h^2}(w_1 - 2w_0 + w_{-1}) = \frac{2}{h^2}w_1 \qquad (40)$$

and

$$w_o = 0 \tag{41}$$

Replacing $\underline{z}^o$ by

$$\left\{ \begin{array}{c} \dfrac{2}{h^2} w_1 \\ 0 \end{array} \right\}$$

the matrix equation for $i = 1$ in (36) becomes:

$$\left[\begin{array}{cc} -2\left(1 - \dfrac{h^p}{T}\right) + h^2\left\{\lambda^2 - p(p-1)\dfrac{h^{p-2}}{T}\right\}, & \dfrac{2}{h^2}\left\{1 - \dfrac{1}{T}(h^p - ph^p)\right\} \\ -h^2 & , & -2 \end{array} \right] \underline{z}^1 \tag{42}$$

$$+ \left[\begin{array}{cc} 1 - \dfrac{1}{T}(h^p + ph^p) , & 0 \\ 0 & , & 1 \end{array} \right] \underline{z}^2 = \left\{ \begin{array}{c} 0 \\ 0 \end{array} \right\}$$

Since w_n and η_n are both zero ($w'' = 0$, $w = 0$ at $x = 1$), $\underline{z}^n$ is a zero matrix. Then

$$\begin{bmatrix} 1 - \frac{1}{T}\left\{(n-1)^n h^n - nh\,(n-1)^{n-1} h^{n-1}\right\}, & 0 \\ 0, & 1 \end{bmatrix} \underline{z}^{n-2} \qquad (43)$$

$$+ \begin{bmatrix} -2\left(1 - \frac{1}{T}(n-1)^n h^n\right) + h^2\left\{\lambda^2 - \frac{n(n-1)}{T}(n-1)^{n-2} h^{n-2}\right\}, & 0 \\ -h^2, & ,-2 \end{bmatrix} \underline{z}^{n-1} = \begin{Bmatrix} 0 \\ 0 \end{Bmatrix}$$

Since the matrix equation obtained is banded along the diagonal, it can be conveniently treated by Potter's method (Reference [13]), but it should be noted here that to remove the singular behavior of the determinant, a slight modification is necessary (Reference [14]).

Calculation of the buckling load according to the finite difference formulation derived was done on UNIVAC 1108 computer. The computer program is given in Appendix F .

Consideration of the Simply Supported Beam

Determination of Absolute Values of End Slopes

The simply supported beam shown in Figure 8 is considered. The variation of the bending stiffness is of the same form as (3). First the sum of the absolute values of the slope at both ends under a uniformly distributed load is treated.

Linear Variation in Stiffness (p = 1). Since $w'' = 0$ at $x = 0$

and 1, constants A and B in equation (5) can be determined easily. Thus for this case

$$(T - x) \frac{w''}{T} = \frac{1}{2} (x^2 - x) \tag{44}$$

Hence

$$2 \frac{w''}{T} = - (T - 1) - x + T(T - 1) \frac{1}{T-x} \tag{45}$$

Integration of (45) yields,

$$\frac{2}{T} w' = - \frac{x^2}{2} - (T - 1)x - T(T - 1)\ln(T - x) + C \tag{46}$$

where C is a constant. From (46) the algebraic difference of the end slopes is obtained. It is

$$(w'_{x=1} - w'_{x=0}) = \frac{T}{2} \left[\frac{1}{2} - T + T(T-1)\ln(\frac{T}{T - 1}) \right] \tag{47}$$

Parabolic Variation in Stiffness (p = 2). Define $\Lambda^2 = T$, then

$$(\Lambda^2 - x^2) \frac{w''}{T} = \frac{1}{2}(x^2 - x) \tag{48}$$

Equation (48) can be rewritten as

$$\frac{2}{T} w'' = -1 + \frac{\Lambda+1}{2} \frac{1}{\Lambda+x} + \frac{\Lambda-1}{2} \frac{1}{\Lambda-x} \tag{49}$$

Integration of (49) gives

$$\frac{2}{T} w' = -x + \frac{\Lambda+1}{2} \ln(\Lambda+x) - \frac{\Lambda-1}{2} \ln(\Lambda-x) + C$$

Where C is a constant. Hence

$$\frac{2}{T}(w'_{x=1} - w'_{x=0}) = -1 + \frac{\Lambda}{2} \ln(\frac{\Lambda+1}{\Lambda-1}) + \frac{1}{2} \ln(\frac{T-1}{T})$$

or

$$w'_{x=1} - w'_{x=0} = \frac{T}{2}[-1 + \frac{\sqrt{T}}{2} \ln(\frac{\sqrt{T}+1}{\sqrt{T}-1}) + \frac{1}{2} \ln(\frac{T-1}{T})] \tag{50}$$

Formulation of Finite Difference Equations for Buckling Load Determination

The finite difference formulation and the boundary matrix at x = 1 are the same as for the clamped-pinned case. The only change required is the boundary matrix at x = 0. Equation (42) is to be replaced by the following matrix equation:

$$
\left[
\begin{array}{cc}
-2\left(1 - \dfrac{h^p}{T}\right) + h^2\left\{\lambda^2 - p(p-1)\,\dfrac{h^{p-2}}{T}\right\}, & 0 \\[2em]
-h^2 & , \quad -2
\end{array}
\right] \underline{z}^1
$$

$$
+ \left[
\begin{array}{cc}
1 - \dfrac{1}{T}(h^p + ph^p), & 0 \\[2em]
0 & , \quad 1
\end{array}
\right] \underline{z}^2 = \left\{
\begin{array}{c}
0 \\[1em]
0
\end{array}
\right\} \tag{51}
$$

APPENDIX E

CANTILEVER WITH TIP LATERAL SPRING

Characteristic Equation for Instability

The buckling load of a cantilever beam with a lateral tip spring (Figure 5) is to be calculated from the characteristic equation.

The non-dimensionalized differential equation is

$$w^{IV} + \lambda^2 w'' = 0 \qquad (1)$$

And the appropriate boundary conditions are

$$w = w' = 0 \qquad \text{at} \quad x = 0 \qquad (2)$$

$$w'' = w''' + \lambda^2 w' - \beta_1 w = 0 \quad \text{at} \quad x = 1$$

Thus the general solution is obtained as

$$w = A \sin \lambda x + B \cos \lambda x + Cx + D \qquad (3)$$

Fulfillment of the boundary conditions (2) by the general solution yields the following equation:

$$
\begin{bmatrix}
\sin \lambda & \cos \lambda \\
-\lambda^3 - \beta_1 (\sin \lambda - \lambda) & -\beta_1 (\cos \lambda - 1)
\end{bmatrix}
\begin{Bmatrix} A \\ B \end{Bmatrix}
= \begin{Bmatrix} 0 \\ 0 \end{Bmatrix}
\tag{4}
$$

By equating the determinant value of coefficient matrix in equation (4) to zero, the buckling equation is obtained; viz

$$
\begin{vmatrix}
\sin \lambda & \cos \lambda \\
-\lambda^3 - \beta_1 (\sin \lambda - \lambda) & -\beta_1 (\cos \lambda - 1)
\end{vmatrix}
= 0
\tag{5a}
$$

Expanding the determinant, the following characteristic equation is obtained:

$$
\beta_1 (\sin \lambda - \lambda \cos \lambda) + \lambda^3 \cos \lambda = 0
\tag{5b}
$$

From equation (4),

$$
B = - A \tan \lambda
$$

Using this result and boundary conditions at $x = 0$ of equation (2) in equation (3), the buckled mode shape is:

$$
w(x) = A\{\sin \lambda x - \lambda x - \tan \lambda (\cos \lambda x - 1)\}
\tag{6}
$$

Behavior Under a Concentrated Lateral Force

A concentrated lateral force is applied to the cantilever beam

with a lateral spring (Figure). The deflection under this loading is to be derived.

Non-dimensionalized differential equation is

$$w^{IV} - \bar{Q}\delta(x - \zeta) = 0 \tag{7}$$

where $\delta(x)$ is a Dirac delta function. Boundary conditions are:

$$\text{at } x = 0 \qquad w = w' = 0$$
$$\text{at } x = 1 \qquad w'' = w''' - \beta_1 w = 0$$

Let the operator of Laplace transformation be denoted by $L(\ )$. Defining $w(s) = L(w(x))$, equation (7) can be transformed in the following form:

$$s^4 w(s) - \{s^3 w(0) + s^2 w'(0) + s w''(0) + w'''(0)\} - \bar{Q}e^{-\zeta s} = 0 \tag{8}$$

Noting that $w(0)$ and $w'(0)$ are zero, equation (8) can be transformed back as follows:

$$w = Ax^3 + Bx^2 = w_1(x) \qquad 0 \le x \le \zeta \tag{9}$$

$$w = w_1(x) + \frac{\bar{Q}}{6}(x - \zeta)^3 \qquad \zeta \le x \le 1$$

Two constants A, B are evaluated from the boundary conditions. They are,

$$A = - \frac{\bar{Q}}{4(\beta_1+3)} \left[\beta_1(1-\zeta) - \frac{\beta_1}{3}(1-\zeta)^3 + 2\right] \qquad (10)$$

$$B = \frac{\bar{Q}}{4(\beta_1+3)} \left[\beta_1(1-\zeta) - \beta_1(1-\zeta)^3 + 6\zeta\right]$$

Behavior Under Uniformly Distributed Lateral Force

A uniformly distributed lateral load is applied to a cantilever beam with a tip spring as shown in Figure 5. The distribution of shear force, bending moment, in addition to slope and deflection are to be derived.

The non-dimensionalized differential equation is

$$w^{IV} - \bar{q} = 0 \qquad (11)$$

Boundary conditions are the same as the previous case. Integrating (11) in succession and satisfying the boundary conditions yields the following results:

$$w''' = \bar{q} \left[x - \frac{5\beta_1 + 24}{8(\beta_1 + 3)}\right] \qquad (12a)$$

$$w'' = \frac{\bar{q}}{8} \left[4x^2 - \frac{5\beta_1 + 24}{\beta_1 + 3} x + \frac{\beta_1 + 12}{\beta_1 + 3}\right] \qquad (12b)$$

$$w' = \frac{\bar{q}}{48} \left[8x^3 - \frac{3(5\beta_1 + 24)}{\beta_1 + 3} x^2 + 6 \frac{\beta_1 + 12}{\beta_1 + 3} x\right] \qquad (12c)$$

$$w = \frac{\bar{q}}{48} \left[2x^4 - \frac{5\beta_1 + 24}{\beta_1 + 3} x^3 + 3 \frac{\beta_1 + 12}{\beta_1 + 3} x^2 \right] \qquad (12d)$$

From (12b), the locations of zero-moment are given by

$$4x^2 - \frac{5\beta_1 + 24}{\beta_1 + 3} x + \frac{\beta_1 + 12}{\beta_1 + 3} = 0 \qquad (13)$$

$$x_1 = 1, \qquad x_2 = \frac{\beta_1 + 12}{4(\beta_1 + 3)}$$

Hence, the distance between inflection points is

$$\bar{\ell}_{ext} = x_2 - x_1 = \frac{3\beta_1}{4(\beta_1 + 3)} \qquad (14)$$

and the location of zero shearing force is

$$x_o = \frac{5\beta_1 + 24}{8(\beta_1 + 3)} \qquad (15)$$

Behavior Under a Concentrated Tip Couple

A concentrated couple is applied to a cantilever beam with a lateral tip spring (Figure 5).

The deflection due to a couple can be obtained by differentiating the deflection due to a unit lateral load with respect to the coordinate ζ where the lateral load is applied. Thus, differentiating

equation (9) with respect to ζ gives

$$w = Cx^3 + Dx^2 = \bar{w}(x) \qquad 0 \le x < \zeta \qquad (16)$$

$$w = \bar{w}(x) - \frac{\bar{\mu}}{2}(x - \zeta)^2 \qquad \zeta \le x \le 1$$

where

$$C = - \frac{\bar{\mu}}{4(\beta_1 + 3)}\left[-\beta_1 + \beta_1(1 - \zeta)^2\right] \qquad (17)$$

$$D = \frac{\bar{\mu}}{4(\beta_1 + 3)}\left[-\beta_1 + 3\beta_1(1 - \zeta)^2 + 6\right]$$

Especially when a couple is applied at the tip, the deflection becomes

$$w(x) = \frac{\bar{\mu} x^2}{4(\beta_1 + 3)}\left\{\beta_1 x + (6 - \beta_1)\right\} \qquad (18)$$

Slope at the tip due to an end couple is

$$w'(1) = \frac{\bar{\mu}}{4(\beta_1 + 3)}\left[3\beta_1 + 2(6-\beta_1)\right] = \frac{\beta_1 + 12}{4(\beta_1+3)}\bar{\mu} \qquad (19)$$

APPENDIX F

COMPUTER PROGRAMS

```
C.....BEAM WITH ROTATIONAL SPRINGS AT BOTH ENDS. FIND PCRT. FIND RATIO
C.....OF LENGTH UPTO THE INFLEXION POINT FROM THE OPPOSITE END OF THE
C.....BEAM TO THE SLOPE AT THAT POINT.FIND PRODUCT OF THIS RATIO AND
C.....PCRT.
      DIMENSION         BTA(40), PEX(40),AL3(40),P3(40),ERROR3(40)
      REAL L,LLOW,LUP,LNEW
      DATA( BTA (I),I=1,27)/0.,.25,.5,75,1.,1.5,2.,2.5,3.,3.5,4.,4.5,5.
     1,5.5,6.,6.5,7.,7.5,10.,20.,50.,100.,500.,1000.,5000.,10000.,100000
     1.0/
C.....CYCLE FOR BETA1
      DO 10 I=1,27
      WRITE (6,140)
  140 FORMAT(1H1,10H   BETA1,10H   BETA2,10H   PCRT,10H   L1/24*  1
     1,10H   ERROR1,10H   L2/24* 2,10H   ERROR2,10H   LEXT,10H
     1PEXT,10H   ERROR//)
      DO 15 M=1,27
C.....CYCLE FOR BETA2
      C=12.0+4.0*(BTA(I)+BTA(M))+BTA(I)*BTA(M)
      B1=BTA(I)+BTA(M)
      B2=BTA(I)*BTA(M)
C.....CYCLE FOR FINDING L(=PEX(I)),WHEN CHARACTERISTIC EQN. IS SATISFIED
   30 DO 40 K=1,600
      L=FLOAT(K)-0.9
      DET=B1*(SIN(L)-L*COS(L))/(L*L)
      DET=DET+B2*(2.0-2.0*COS(L)-L*SIN(L))/(L*L*L)+SIN(L)
  200 IF(K.EQ.1) GO TO 60
      IF(D1*DET)50,50,60
   50 DLOW=D1
      DUP=DET
      LUP=L
C.....BISECTION SCHEME STARTS.
   70 LNEW=LLOW+DLOW*(LUP-LLOW)/(DLOW-DUP)
      DIF1=LNEW-LLOW
      DIF2=LUP-LNEW
      IF(DIF1.LT.0.0005.OR.DIF2.LT.0.0005) GO TO 100
      DET=B1*(SIN(LNEW)-LNEW*COS(LNEW))/(LNEW*LNEW)+SIN(LNEW)
      DET=DET+B2*(2.0-2.0*COS(LNEW)-LNEW*SIN(LNEW))/(LNEW)**3
      IF(DET*DLOW) 80,80,90
   80 DUP=DET
      LUP=LNEW
      GO TO 70
```

```
   90 DLOW=DET
      LLOW=LNEW
      GO TO 70
   60 D1=DET
      LLOW=L
   40 CONTINUE
C.....BISECTION SCHEME ENDS.
  100 PEX(I)=LNEW*LNEW/9.8696
C.....TO OBTAIN THE INFLEXION POINTS X1,X2.
      A=6.0
      B=-6.0*(1.0+(BTA(I)-BTA(M))/C)
      D=BTA(I)*(BTA(M)+6.0)/C
      E=SQRT(B*B-4.0*A*D)
      X1=-(B+E)/12.0
      X2=(-B+E)/12.0
C.....AL1=LENGTH BETWEEN LEFT END AND 2ND INFLEXION POINT.
      AL1=X2
C.....AL2=LENGTH BETWEEN RIGHT END AND 1ST INFLEXION POINT.
      AL2=1.0-X1
C.....THETA1=SLOPE AT AL1.
      THETA1=(2.0*X2**3+X2*X2*B/2.0+D*X2+(BTA(M)+6.0)/C)/12.0
C.....THETA2=SLOPE AT AL2.
      THETA2=(2.0*X1**3+X1*X1*B/2.0+D*X1+(BTA(M)+6.0)/C)/12.0
      P1=AL1/(24.0*THETA1)
      P2=AL2/(24.0*THETA2)
      P1=ABS(P1)
      P2=ABS(P2)
      ERROR1=(P1-PEX(I)*100.0/PEX(I)
      ERROR2=(P2-PEX(I)*100.0/PEX(I)
      AL3(M)=X2-X1
      P3(M)=(1.0+AL3(M))/(2.0*AL3(M)**3)
      ERROR3(M)=(P3(M)-PEX(I))*100.0/PEX(I)
   15 WRITE (6,51) BTA(I),BTA(M),PEX(I),P1,ERROR1,P2,ERROR2,AL3(M),P3(M),
     1ERROR3(M)
   51 FORMAT(2F10.2,8F10.6/)
   10 CONTINUE
      STOP
      END
```

```
C.....FINITE DIFFERENCE METHOD FOR BUCKLING OF A CLAMPED-PINNED BEAM
C.....OF VARIABLE EI.
      DIMENSION A(2,2),B(2,2)
      COMMON N,H,X,A,B,TAPER,POWER,HSQR
      TAPER=3
      POWER=2.
      DATA((A(I,J),I=1,2),J=1,2)/1.0,0.,0.,1.0/
      DATA(N1,N2,N3,L1,L2,L3)/10,30,5,1,51,10/
      DO 30 N=N1,N2,N3
      H=1.0/N
      HSQR=H*H
      DO 40 L=L1,L2,L3
      X=FLOAT(L)
      IF(L.GT.(L2-1)) GO TO 20
      CALL DETERM(DET0,DET2)
       IF(L.EQ.L1) GO TO 50
      IF(DET1*DET2) 60,60,70
   50 DET1=DET0
      GO TO 40
   70 DET1=DET2
      GO TO 40
   60 DETLOW=DET1
      DETUP=DET2
      XLOW=X-L3
      XUP=X
      GO TO 400
   80 IF(DETLOW*DET2) 85,85,90
   85 DETUP=DET2
      XUP=X
      GO TO 400
   90 DETLOW=DET2
      XLOW=X
      GO TO 400
   20 WRITE(6,100)
  100 FORMAT(1H1,12H NO SOLUTION)
      GO TO 30
C.....SUBPROGRAM FOR BISECTION.
  400 X=XLOW+DETLOW/(DETLOW-DETUP)*(XUP-XLOW)
      DIF1=ABS(X-XLOW)
      DIF2=ABS(X-XUP)
      IF(DIF1.LT.0.01.OR.DIF2.LT.0.01) GO TO 200
      CALL DETERM(DET0,DET2)
      GO TO 80
C.....END OF BISECTION PROGRAM.
   40 CONTINUE
  200 X=X/9.8696
      WRITE(6,300)N,X
  300 FORMAT(      I5,2F15.6/)
   30 CONTINUE
      STOP
      END
```

```
      SUBROUTINE DETERM(DETO,DET2)
      DIMENSION A(2,2),B(2,2),P(2,2),AP(2,2),BAP(2,2),V(2),JC(4)
      DIMENSION LB1(2,2),LB2(2,2),RB1(2,2),RB2(2,2)
      COMMON N,H,X,A,B,TAPER,POWER,HSQR
      REAL LB1,LB2,JC
      LB1(1,1)=-2.0*(1.0-(H**POWER)/TAPER)+X*HSQR
      LB1(1,2)=2.0*(1.0-(H**POWER)/TAPER)/HSQR
      LB1(2,1)=-HSQR
      LB1(2,2)=-2.0
      A(1,1)=1.0-(H**POWER)/TAPER
      C=LB1(1,1)*LB1(2,2)-LB1(1,2)*LB1(2,1)
      DO 500 I=1,2
      DO 500 J=1,2
  500 LB2(I,J)=A(I,J)
      B(1,2)=0.
      B(2,1)=-HSQR
      B(2,2)=-2.0
      V(1)=1.0
      CALL GJR(LB1,2,2,2,2,$350,JC,V)
      CALL MXMLT(LB1,LB2,P,2,2,2,2,2)
      DSIGN=C/ABS(C)
      N4=N-3
      DO 280 M=1,N4
      A(1,1)=(1.0-((M+1.0)*H)**POWER/TAPER)
      B(1,1)=-2.0*A(1,1)+X*HSQR
      CALL MXMLT(A,P,AP,2,2,2,2,2)
      CALL MXSUB(B,AP,BAP,2,2,2)
      C=BAP(1,1)*BAP(2,2)-BAP(1,2)*BAP(2,1)
      V(1)=1.0
      CALL GJR(BAP,2,2,2,2,$350,JC,V)
      CALL MXMLT(BAP,A,P,2,2,2,2,2)
      U=C/ABS(C)
  280 DSIGN=DSIGN*U
      A(1,1)=1.0-((N-1.0)*H)**POWER/TAPER
      B(1,1)=-2.0*(1.0-((N-1.0)*H)**POWER/TAPER)+X*HSQR
      DO 550 I=1,2
      DO 550 J=1,2
      RB1(I,J)=A(I,J)
  550 RB2(I,J)=B(I,J)
      CALL MXMLT(RB1,P,AP,2,2,2,2,2)
      CALL MXSUB(RB2,AP,BAP,2,2,2)
      Y=BAP(1,1)*BAP(2,2)-BAP(1,2)*BAP(2,1)
      DETO=DSIGN*Y
      DET2=DETO
  350 RETURN
      END
```

```
C.....FINITE DIFFERENCE METHOD FOR BUCKLING OF A S.S.BEAM
C.....OF VARIABLE EI.
      DIMENSION A(2,2),B(2,2)
      COMMON  N,H,X,A,B,TAPER,POWER,HSQR
      TAPER=3.
      POWER=2.
      DATA((A(I,J),I=1,2),J=1,2)/1.0,0.,0.,1.0/
      DATA(N1,N2,N3,L1,L2,L3)/10,30,5,1,51,10/
      DO 30 N=N1,N2,N3
      H=1.0/N
      HSQR=H*H
      DO 40 L=L1,L2,L3
      X=FLOAT(L)
      IF(L.GT.(L2-1)) GO TO 20
      CALL DETERM (DET0,DET2)
       IF(L.EQ.L1) GO TO 50
      IF(DET1*DET2) 60,60,70
   50 DET1=DET0
      GO TO 40
   70 DET1=DET2
      GO TO 40
   60 DETLOW=DET1
      DETUP=DET2
      XLOW=X-L3
      XUP=X
      GO TO 400
   80 IF(DETLOW*DET2) 85,85,90
   85 DETUP=DET2
      XUP=X
      GO TO 400
   90 DETLOW=DET2
      XLOW=X
      GO TO 400
   20 WRITE(6,100)
  100 FORMAT(1H1,12H NO SOLUTION)
      GO TO 30
C.....SUBPROGRAM FOR BISECTION.
  400 X=XLOW+DETLOW/(DETLOW-DETUP)*(XUP-XLOW)
      DIF1=ABS(X-XLOW)
      DIF2=ABS(X-XUP)
      IF(DIF1.LT.0.01.OR.DIF2.LT.0.01)GO TO 200
      CALL DETERM(DET0,DET2)
      GO TO 80
C.....END OF BISECTION PROGRAM.
   40 CONTINUE
  200 X=X/9.8696
      WRITE (6,300) N,X
  300 FORMAT(      I5,2F15.6/)
   30 CONTINUE
      STOP
      END
```

```
      SUBROUTINE DETERM(DETO,DET2)
      DIMENSION A(2,2),B(2,2),P(2,2),AP(2,2),BAP(2,2),V(2),JC(4)
      DIMENSION LB1(2,2),LB2(2,2),RB1(2,2),RB2(2,2)
      COMMON N,H,X,A,B,TAPER,POWER,HSQR
      REAL LB1,LB2,JC
      LB1(1,1)=-2.0*(1.0-(H**POWER)/TAPER)+X*HSQR
      LB1(1,2)=0.0
      LB1(2,1)=-HSQR
      LB1(2,2)=-2.0
      A(1,1)=1.0-(H**POWER)/TAPER
      C=LB1(1,1)*LB1(2,2)-LB1(1,2)*LB1(2,1)
      DO 500 I=1,2
      DO 500 J=1,2
  500 LB2(I,J)=A(I,J)
      B(1,2)=0.
      B(2,1)=-HSQR
      B(2,2)=-2.0
      V(1)=1.0
      CALL GJR(LB1,2,2,2,2,$350,JC,V)
      CALL MXMLT(LB1,LB2,P,2,2,2,2,2)
      DSIGN=C/ABS(C)
      N4=N-3
      DO 280 M=1,N4
      A(1,1)=(1.0-((M+1.0)*H)**POWER/TAPER)
      B(1,1)=-2.0*A(1,1)+X*HSQR
      CALL MXMLT(A,P,AP,2,2,2,2,2)
      CALL MXSUB(B,AP,BAP,2,2,2)
      C=BAP(1,1)*BAP(2,2)-BAP(1,2)*BAP(2,1)
      V(1)=1.0
      CALL GJR(BAP,2,2,2,2,$350,JC,V)
      CALL MXMLT(BAP,A,P,2,2,2,2,2)
      U=C/ABS(C)
  280 DSIGN=DSIGN*U
      A(1,1)=1.0-((N-1.0)*H)**POWER/TAPER
       B(1,1)=-2.0*(1.0-((N-1.0)*H)**POWER/TAPER)+X*HSQR
      DO 550 I=1,2
      DO 550 J=1,2
      RB1(I,J)=A(I,J)
  550 RB2(I,J)=B(I,J)
      CALL MXMLT(RB1,P,AP,2,2,2,2,2)
      CALL MXSUB(RB2,AP,BAP,2,2,2)
      Y=BAP(1,1)*BAP(2,2)-BAP(1,2)*BAP(2,1)
      DETO=DSIGN*Y
      DET2=DETO
  350 RETURN
      END
```

```
C.....FINITE NUMBER OF CONCENTRATED LOAD AT EQUALLY SPACED LOCATIONS
C.....TO APPROXIMATE THE UNIFORMLY DISTRIBUTED LOAD ON THE COLUMN
C.....ROTATIONALLY RESTRAINED AT BOTH ENDS.  THE DISTANCE BETWEEN TWO
C.....INFLECTION POINTS IS TO BE CALCULATED.  24 JUNE 1970
      DIMENSION BETA(14)
      REAL JO,NO,LEXT
      INTEGER COUNT
      DATA(BETA(I),I=1,14)/0.0,.1,.5,1.0,2.0,5.0,10.0,20.0,50.0,
     1100.0,500.0,1000.0,10000.0,100000.0/
      DO 20 I=1,14
      DO 25  K=1,14
      BETA1=BETA(I)
      BETA2=BETA(K)
      BETA26=BETA2 +6.0
      BDIF=BETA1-BETA2
      BSUM=BETA1 +BETA2
      BPRO=BETA1 *BETA2
      DELTA=12.0 +4.0*BSUM +BPRO
      LEXT=SQRT((1.0+BDIF/DELTA)**2-2.0*BETA1*BETA26/3.0/DELTA)
      PCRUNI=(1.0 +LEXT)/(2.0*LEXT**3)
      C1=BETA1*BETA26/12.0/DELTA
      C2=(BPRO+5.0*BETA1+3.0*BETA2+12.0)/DELTA
      C3=BETA26*(BETA1 + 2.0)/DELTA
      WRITE(6,200) BETA1,BETA2
      WRITE(6,250)
      DO 10 N=1,20
      NO=FLOAT(N)
      XO=0.0
      J1=0
      COUNT=1
   60 DO 30  J=J1,N
      JO=FLOAT(J)
      XFRONT=JO/(NO+1.0)
      XAFT=(JO+1.0)/(NO+1.0)
      CC=C1*NO*(NO+2.0)/(NO+1.0)-.5*JO*(JO+1.0)/(NO+1.0)
      CX=-.5*NO/(NO+1.0)*(NO*C2+C3)+JO
      X=-CC/CX
      IF((XFRONT-X)*(XAFT-X))40,40,30
   40 Y=X-XO
      XO=Y
      IF(COUNT.EQ.2) GO TO 100
      COUNT=COUNT+1
      J1=J+1
      GO TO 60
   30 CONTINUE
  100 PCRFIN=(1.0+Y)/(2.0*Y**3)
      ERROR=(PCRFIN-PCRUNI)/PCRUNI*100.0
      WRITE(6,300) N,LEXT,PCRUNI,PCRFIN,ERROR
   10 CONTINUE
   25 CONTINUE
```

```
   20 CONTINUE
  200 FORMAT(1H1,12H      BETA1=,F10.2,12H      BETA2=,F10.2//)
  250 FORMAT(4H  NO,11H     LUNI,15H     PCRUNI,
     120H           LFIN,20H           PCRFIN,10H      ERROR//)
  300 FORMAT(I5,5F15.6)
      STOP
      END
```

REFERENCES

1. Salmon, E. H., "Columns, A Treatise on the Strength and Design of Compressive Members", Henry Frowde and Hodder and Stoughton, London, 1921.

2. Niles and Newell, Airplane Structures, Vol. 1, John Wiley and Sons, New York, 1953, p. 350.

3. Horton, W. H., and Struble, D. E., "End Fixity of Columns", USAAVLABS TR 70-10, July 1970, United States Army Aviation Material Laboratories, Fort Eustis, Virginia.

4. Horton, W. H., Cundari, F. L., and Johnson, R. W., "The Analysis of Experimental Data Obtained From Stability Structures on Elastic Column and Plate Structures", Israel Journal of Technology, Vol. 5, No. 1-2, 1967, pp. 104-113.

5. Fisher, H. R., "An Extension of Southwells Method of Analyzing Experimental Observations in Problems of Elastic Stability", Proceedings of the Royal Society of London, Series A, 144, p. 609-630, 1934.

6. Massonet, C., "Les Relations entre les Modes Normaux de Vibration et la Stabilité des Systemés Élastiques", Goemaere, Bruxelles, 1940.

7. Horton, W. H., Craig, J. I., and Struble, D. E., "A Simple, Practical Method for the Experimental Determination of the End Fixity of a Column", Proceedings of the 8th International Symposium on Space Technology and Science, Aug. 1969, Tokyo, Japan.

8. Horton, W. H., and Ford, J. S., II, "Some Experimental Studies on the Relationship Between End Fixity and Critical Load Level for Struts", USAAVLABS TR 70-21, July 1970, United States Army Aviation Material Laboratories, Fort Eustis, Virginia.

9. Struble, D. E., "Boundary Effects in Structural Stability: A New Approach", Ph.D. Thesis, January 1970, Georgia Institute of Technology, Atlanta, Georgia.

10. Baruch, M., "On Undestructive Determination of the Buckling Load of an Elastic Bar", GITAER 70-1, March 1970, Georgia Institute of Technology, Atlanta, Georgia.

11. Pippard, A. J. S., and Pritchard, J. L., "Aerosplane Structures", Longmans Green and Company, London, 1936, p. 103.

12. Collatz, L., "The Numerical Treatment of Differential Equation", Springer Verlag, Berlin, 1960.

13. Potters, M. L., "A Matrix Method for the Solution of a Second Order Differential Equation in Two Variables", <u>Mathematisch Centrum,</u> Amsterdam, Holland, Report MR 19,1955.

14. Robert, E. B., and Robert, E. F., "A Modification of Potters Method for Solving Eigenvalue Problems Involving Triagonal Matrices", <u>AIAA Journal,</u> December 1966, p. 2231-2232.

15. Wang, C. T., "Applied Elasticity", McGraw-Hill, New York, 1953, p. 269.

16. Courant, R., and Hilbert, D., "Methods of Mathematical Physics - Volume 1", Interscience, New York, 1953.

17. Livesley, R. F., and Chandler, D. B., "Stability Functions for Structural Frameworks," Manchester Univ. Press, 1956.

VITA

Takaya Iwamoto was born March 25, 1942 in Eishokodo, Manchuria. He is a Japanese citizen and completed his secondary education in Nobeoka, Japan in 1960.

Mr. Iwamoto studied aeronautics at the University of Tokyo and graduated in 1964. Subsequently, he was employed by Kawasaki Aircraft Company, Ltd. as a research engineer. After working in many diversified areas he decided to pursue a graduate degree in the field of Aerospace Structures, and entered graduate school at the Georgia Institute of Technology in September 1967. He was a research assistant there until June 1971.

He is married and presently resides in Kakamigahara, Gifu, Japan where he is employed in research and development by Kawasaki Heavy Industry, Ltd.